LINE-1 retrotransposition in neuronal cells

The identification of TNPO1 and TNPO3 as host factors of LINE-1 retrotransposition

THESIS

submitted by

Laura DEBUSSCHERE

Laboratory of Molecular Virology and Gene Therapy

Academic promoter: Prof. Dr. Zeger DEBYSER

Supervisor: Saskia LESIRE

LEUVEN

Academic year 2020-2021

DANKWOORD - ACKNOWLEDGEMENTS

Na 8 maanden intensief onderzoek naar LINE-1 retrotranspositie, ben ik fier op het eindresultaat van deze masterproef. Natuurlijk is deze masterproef het resultaat van de inbreng van verschillende personen, die ik graag even zou willen bedanken.

Bedankt aan mijn promoter, prof. Dr. Zeger Debyser, om me de kans te geven mijn masterproef in uw laboratorium af te leggen. Uw gedrevenheid en passie voor onderzoek werken aanstekelijk om zelf ook kwalitatief onderzoek te verrichten. Bedankt voor uw enthousiasme over de bekomen resultaten tijdens de minimeetings en het geven van nieuwe ideeën om bepaalde resultaten te verklaren. Ook bedankt voor de begeleiding tijdens het schrijven van de masterproef.

Dankjewel aan mijn supervisor, Saskia Lesire, voor de super begeleiding tijdens het experimenteel werk en het schrijven van mijn masterproef. Dankjewel om altijd klaar te staan om bepaalde zaken te verduidelijken en voor je geduld met mij. Dankjewel om mijn masterproef meermaals na te lezen en suggesties te geven. Chapeau hoe je mij de afgelopen 8 maanden intensief hebt begeleid en dit allemaal tijdens je eerste jaar van je doctoraat!

Ik wil ook graag het volledige LEDGF team bedanken om me direct thuis te laten voelen in de groep. Ook bedankt voor jullie suggesties en constructieve feedback tijdens de minimeetings. Thank you Dr. Frauke Christ for your help and advice during the minimeetings. Ook dankjewel aan Nam Joo voor de hulp bij de optimalisatie van de stainings. Bedankt Dr. Chris Van Den Haute om altijd bereid te zijn te helpen en me te helpen met nieuwe inzichten te creëren. Bedankt Joris en Dr. Wouter Peelaerts om te helpen met het microscoopwerk.

Dankjewel mama en papa om me de kans te geven mijn droom te verwezenlijken en me altijd te steunen! Dankjewel zus om ervoor te zorgen dat ik ook voldoende ontspanning nam! Dankjewel Matts om me altijd op te vangen ook wanneer ik niet de meest aangename persoon was en voor de geruststellende dikke knuffels!

TABLE OF CONTENTS

LIST OF ABBREVIATIONS

AD   Alzheimer's disease

AGS   Aicardi-Goutières syndrome

Amp^R Resistance to ampicillin

AT   Ataxia-telangiectasia

ATM   Ataxia-telangiectasia mutated

BsdR   Blasticidin resistance gene

C   Cysteine rich

CDS   Coding sequence

CMV   Cytomegalovirus

CNV   Copy number variant

DAB   3,3-diaminobenzidine

DMEM   Dulbecco's modified Eagle medium

EBNA-1   Epstein-Barr virus nuclear antigen 1

EGFP   Enhanced green fluorescent protein

EN   Endonuclease

FBS   Fetal bovine serum

GAPDH   Glyceraldehyde 3-phosphate dehydrogenase

GFP   Green fluorescent protein

HDAC1   Histone deacetylase 1

HERVs   Human endogenous retroviruses

HIV-1   Human immunodeficiency virus type 1

IFN-1   Type I interferon

JM111   99-JM111-EGFP-Puro plasmid

KD   Knock-down

L1RP   99-L1RPS-EGFP-Puro plasmid

LINE-1   Long interspersed nuclear element-1

LRRK2   Leucine-rich repeat kinase 2

LTR   Long-terminal repeats

LUHMES   Lund Human Mesenphalic

mDA   Mesencephalic dopaminergic

MeCP2   Methyl-CpG binding protein 2

MFI	Median fluorescence intensity
miRNA	MicroRNA-30
miRNA-128	MicroRNA-128
MPP+	1-methyl-4-phenylpyridinium
MPTP	1-methyl-4-phenyl-1,2,3,6-tetrahydropyridine
NNRTIs	Non-nucleoside RT inhibitors
NPCs	Neuronal progenitor cells
NRTIs	Nucleoside analogue RT inhibitors
NtRTIs	Nucleotide analogue RT inhibitors
ORF1p	ORF1 protein
ORF2p	ORF2 protein
ORFs	Open reading frames
ori	E. Coli origin of replication
OriP	Epstein-Barr virus origin of replication
PBS	Phosphate buffered saline solution
PD	Parkinson's disease
Poly(A)	Polyadenine
Puro^R	Resistance to puromycin
qPCR	Quantitative polymerase chain reaction
RC-LINE-1s	Retrotransposition-competent LINE-1s
RNP	Ribonucleoprotein particle
RT	Reverse transcriptase
RT-qPCR	Real-time quantitative polymerase chain reaction
RUNX3	Runt-related transcription factor 3
SAMHD1	SAM and HD domain-containing deoxynucleoside triphosphate triphosphohydrolase 1
SD	Standard deviation
SDS	Sodium dodecyl sulfate
SFFV	Spleen focus forming virus
shRNA	Short hairpin RNA
SINE	Short interspersed nuclear elements
SIRT6	Sirtuin 6
SIV	Simian immunodeficiency virus
Sox	Sex determining-region Y-box
SR	Serine/arginine-rich
TCF-LEF	Transcription factor-lymphoid enhancer factor

TH	Tyrosine hydroxylase
TNPO1	Transportin-1
TNPO3	Transportin-3
TPRT	Target-primed reverse transcription
TREX1	Three prime repair exonuclease 1
TRN-SR2	Transportin-3
UTR	Untranslated region
WPRE	Woodchuck hepatitis virus post-transcriptional regulatory element
WT	Wild-type
YY1	Ying-Yang factor 1

SUMMARY

The human genome is continually changing, for instance by the introduction of mobile DNA. Retrotransposons are an important class of mobile elements, of which the long interspersed nuclear element-1 (LINE-1) is still active. It is estimated that 17 % of the human genome consists of LINE-1 copies. However, the majority are no longer able to undergo retrotransposition. In humans, between 80 and 100 LINE-1 copies are still active and contribute to the dynamic shaping of the genome. There is an expanding interest in studying the role of LINE-1 in neurological diseases. But, a better insight into the process of LINE-1 retrotransposition and the role of host factors is needed.

The LINE-1 retrotransposition assay in cultured cells allows to investigate the role of host factors in LINE-1 retrotransposition. In the first part of this master thesis, the role of transportin-1 (TNPO1) and transportin-3 (TNPO3) in LINE-1 retrotransposition was investigated. It was hypothesised that they are involved in the nuclear import of the LINE-1 ribonucleoprotein particle complex. Depletion of TNPO1 or TNPO3 in HEK293T cells resulted in a decrease in LINE-1 retrotransposition, supporting the hypothesis that TNPO1 and TNPO3 are host factors of LINE-1. The results obtained for TNPO1 confirm published results while the results in TNPO3 depleted cells are the first to show a potential role of TNPO3 in LINE-1 retrotransposition.

In the past, it was evidenced that LINE-1 retrotransposition takes place in the brain and contributes to the development of neurological diseases. Therefore, it is of relevance to optimize the LINE-1 retrotransposition assay in a neuronal cell line. In this thesis, different approaches were taken to optimize the transfection efficiency in SH-SY5Y cells. However, both liposome-mediated transfection and nucleofection did not result in the desired outcome. Here, a new method was used to estimate the transfection efficiency of the LINE-1 plasmid instead of a smaller reporter plasmid. Further optimization of the transfection is needed to be able to carry out the LINE-1 retrotransposition assay in SH-SY5Y cells.

In order to study the potential role of LINE-1 retrotransposition in the pathogenesis of Parkinson's disease, detection of the ORF1 protein (ORF1p) in the mouse brain is desired. In the last part of this master thesis, we performed an optimization of the immunohistochemical and immunofluorescent staining for the ORF1p in brain slices of wild-type mice. Double staining for the ORF1p and tyrosine hydroxylase in the substantia nigra, revealed a high expression of the ORF1p in all dopaminergic neurons. Since the staining is now optimized in wild-type mice, it is possible to investigate the expression of the ORF1p in different Parkinson's disease mouse models.

SAMENVATTING

Het humaan genoom is continu onderhevig aan verandering, zoals de insertie van mobiel DNA. Retrotransposons vormen een belangrijke klasse van mobiele elementen, waarvan long interspersed nuclear element-1 (LINE-1) nog steeds actief is. Ongeveer 17% van het menselijke genoom bestaat uit LINE-1 kopieën, waarvan de meerderheid geen retrotranspositie meer kan ondergaan. In de mens zijn er ongeveer 80 tot 100 kopieën actief die bijdragen aan de dynamische vormgeving van het genoom. Er is toenemende interesse in het bestuderen van de rol van LINE-1 in neurologische aandoeningen, maar het proces van LINE-1 retrotranspositie en de betrekking van gastfactoren in LINE-1 retrotranspositie moet beter begrepen worden.

De LINE-1 retrotranspositie test in celculturen laat toe om de rol van gastfactoren te bestuderen. In het eerste deel van deze masterproef werd de rol van transportin-1 (TNPO1) en transportin-3 (TNPO3) onderzocht. Er werd verondersteld dat beide betrokken zijn in de nucleaire import van het LINE-1 ribonucleoproteïne partikel complex. Depletie van TNPO1 of TNPO3 in HEK293T cellen resulteerde in een daling van LINE-1 retrotranspositie, wat de hypothese bevestigt. De resultaten met TNPO1 bevestigen een eerdere publicatie terwijl de resultaten verkregen voor cellen met depletie van TNPO3 voor het eerst een potentiële rol van TNPO3 aantonen.

In het verleden werd aangetoond dat LINE-1 retrotranspositie plaatsvindt in de hersenen en bijdraagt aan de ontwikkeling van neurologische ziekten. Daarom is het van belang om de LINE-1 retrotranspositie test in een neuronale cellijn te optimaliseren. In deze masterproef werden verschillende benaderingen gevolgd om de transfectie-efficiëntie in SH-SY5Y cellen te optimaliseren. Echter, zowel liposoom-gemedieerde transfectie als nucleofectie resulteerden niet in het gewenste resultaat. Hier werd een nieuwe methode gebruikt om de transfectie-efficiëntie van het LINE-1 plasmide in plaats van het kleinere reporter plasmide te schatten. Verdere optimalisatie van de transfectie is nodig om de LINE-1 retrotranspositie test in SH-SY5Y cellen uit te kunnen voeren.

Om de potentiële rol van LINE-1 retrotranspositie in de pathogenese van de ziekte van Parkinson te kunnen bestuderen, is detectie van het ORF1 proteïne (ORF1p) in hersenen van de muis nodig. In het laatste deel van deze masterproef werd de optimalisatie van de immunohistochemische en immunofluorescente kleuring voor het ORF1p op hersencoupes van wild-type muizen uitgevoerd. Bovendien onthulde dubbele kleuring voor het ORF1p en tyrosine hydroxylase in de substantia nigra een hoge expressie van het ORF1p in alle dopaminerge neuronen. Omdat de kleuring nu geoptimaliseerd is in wild-type muizen, is het mogelijk om de expressie van het ORF1p te onderzoeken in verschillende muismodellen van de ziekte van Parkinson.

1 INTRODUCTION

1.1 LINE-1 ELEMENTS

The genome of a human individual is subject to two distinct forms of change, namely reversible epigenetic changes and irreversible alteration of the DNA sequence. The latter is caused by errors during DNA replication and repair or through the introduction of mobile DNA (1). These mobile parts of DNA are called transposons, also called jumping genes (2, 3). Transposons are fragments of nucleic acid. These fragments have the ability to jump from one site in the human genome to another site. Mobilisation occurs via the proteins encoded by their DNA sequences, such as reverse transcriptase or DNA transposase (4). In 1950, Barbara McClintock was the first who discovered transposable elements in maize kernels (5). Most transposable elements are unable to transpose, however, some still can mobilise (6). As a result of the mobilisation and insertion of these transposons, genes are disrupted, leading to the development of diseases (4). The human genome its evolution, structure and function are affected by the presence of mobile DNA (2).

The jumping genes are separated into two different categories. DNA transposons belong to the first class and contain several mutations that make them no longer able to transpose in humans (2). They mobilise via a 'cut-and-paste' mechanism (4) (Table 1.1). Here, their sequence is cut out the genome, catalysed by the transposase enzyme and then integrated elsewhere in the human genome (7). Retrotransposons form the second class of transposons, which are of importance since some are still active. Unlike DNA transposons, mobilisation takes place via a 'copy-and-paste' mechanism (Table 1.1) (8). Copy numbers can accumulate elsewhere in the genome without losing their original location (8). Depending if long-terminal repeats (LTR) are present or absent, an additional division is made within this class. LTR sequences are present in human endogenous retroviruses (HERVs) and together with the mammalian apparent LTR-retrotransposons, they comprise 8 % of the human genome (8) (Table 1.1). HERVs, like DNA transposons, contain almost all mutations and are no longer able to mobilise. Non-LTR retrotransposons include the long interspersed nuclear element-1 (LINE-1), which has nearly 500 000 copies present in the genome of a human individual and comprises approximately 17 % of the sequences present in the human genome (2, 8, 9) (Table 1.1). An estimation of 80 to 100 retrotransposition-competent LINE-1s (RC-LINE-1s) is made in an average human individual (10). However, most copies of LINE-1 have no longer the capacity to undergo retrotransposition because of mutation or fragmentation accumulation, methylation of the promoter and formation of heterochromatin (11). Non-LTR retrotransposons also include short interspersed nuclear elements

(SINE), for example *Alu* (Table 1.1). SINE require proteins encoded by LINE-1 for mobilisation and are non-autonomous (2, 8).

*Table 1.1: Overview of transposable elements in the genome of a human individual. Adapted from: H. Kazazian et al, N. Engl. J. Med., 2017, **377**, 361-370.*

Mobile element	Mechanism of mobilisation	% of human genome		Active?
DNA transposons	'cut-and-paste' mechanism	~ 3 %		No
Retrotransposons	'copy-and-paste' mechanism	HERVs	~ 8 %	Uncertain
		LINE-1s	~ 17 %	Yes
		SINE (*Alu*)	~ 10 %	Yes

1.1.1 Structure of a LINE-1 retrotransposon

A LINE-1 element capable of retrotransposition is 6 kb in length and consists of a 5'- and 3'-untranslated region (UTR), two open reading frames (ORFs) and a polyadenine (poly(A)) tail at the 3' end (Fig. 1.1)(12). The two ORFs encode two proteins, the ORF1 protein (ORF1p) and the ORF2 protein (ORF2p). A 63 bp inter-ORF space separates both ORFs. The ORF1p has RNA-binding and nucleic acid chaperone activities, while ORF2p has endonuclease (EN) and reverse transcriptase (RT) activities (4, 13). In the 5'-UTR, an internal RNA polymerase II promoter is present and enables transcription in the sense and antisense direction. Several transcription factors can bind at specific binding sites in this region (14). Recently, in the antisense orientation in the 5'-UTR, another ORF, ORF0, was identified. This ORF0 protein has been found to increase LINE-1 activity (15).
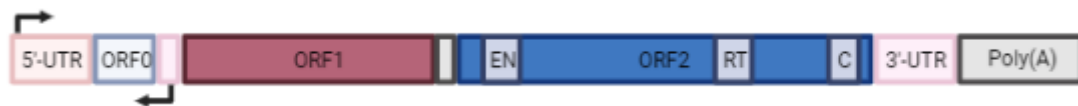
Figure 1.1: Structure of a full-length LINE-1 element. *A full-length LINE-1 element capable of retrotransposition is 6 kb in length and consists of a 5'-UTR that contains a promoter region in the sense and antisense orientation. In the 5'-UTR, ORF0 is present. A LINE-1 element has 2 ORFs, encoding the ORF1p and the ORF2p. ORF2 has an endonuclease (EN), reverse transcriptase (RT) and cysteine rich (C) domain. The 3' end consists of a 3'-UTR and a poly(A) tail. Figure adapted from: H. Kazazian et al, N. Engl. J. Med., 2017, **377**, 361-370.*

1.1.2 Mechanism of LINE-1 retrotransposition

First, a full-length LINE-1 mRNA is produced by the RNA polymerase II promoter region, present in the first 100 base pairs of the 5'-UTR (16). Next, transport of this mRNA to the cytoplasm and translation by ribosomes occur. Consequently, the ORF1p and the ORF2p are expressed and combine with their LINE-1 mRNA to form a ribonucleoprotein particle (RNP) complex. The formation of this RNP complex is an important step in retrotransposition (14). LINE-1 mRNA, trimers of the ORF1p and monomers of

the ORF2p are present in this RNP complex (4). Afterwards, this RNP complex is imported into the nucleus, where integration of this new LINE-1 copy into the genome occurs. The process of integration is known as target-primed reverse transcription (TPRT) (14). At the integration site, the bottom strand of DNA is nicked by the EN encoded by the ORF2p (2). Several analyses have shown that the consensus to cut a strand of genomic DNA is 5'-TTTT/AA-3' (17). As a result, a 3'-OH is exposed at the DNA bottom-strand, which can be used as a primer by the RT enzyme, encoded by the ORF2p (4) (Fig. 1.2).
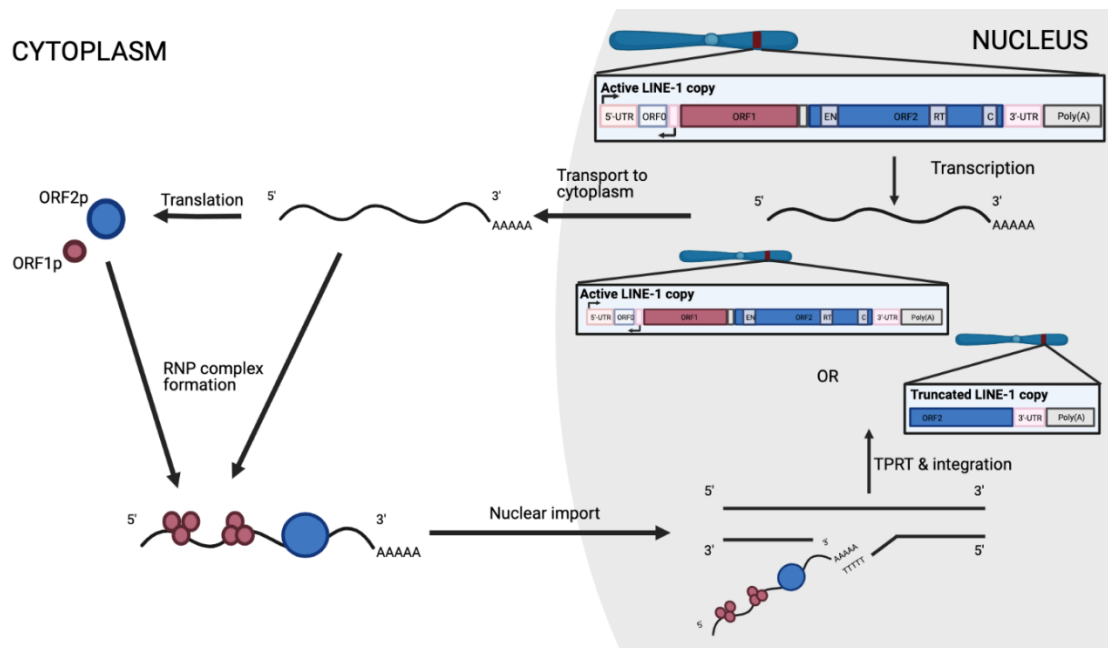
*Figure 1.2: Mechanism of LINE-1 retrotransposition. In the 5'-UTR, the RNA polymerase II promoter region is accountable for the transcription of the DNA to a LINE-1 mRNA. After transport of this mRNA to the cytoplasm, the ORF1p and the ORF2p are encoded. The ORF1p and the ORF2p form together with their LINE-1 mRNA a ribonucleoprotein particle (RNP) complex. After nuclear import of this RNP complex, reverse transcription and integration in the genome happens, known as target-primed reverse transcription (TPRT). The result of a full retrotransposition cycle is an active LINE-1 copy or truncated LINE-1 copy present in the genomic DNA. Figure adapted from: H. Kazazian et al, N. Engl. J. Med., 2017, **377**, 361-370.*

1.2 LINE-1 IN THE BRAIN

Following the discovery of transposable elements in maize kernels by Barbara McClintock in 1950, it was supposed that LINE-1 retrotransposition only occurred in the germline (18). Nevertheless, in 2005, LINE-1 retrotransposition was proven in brain cells, playing a role in genomic mosaicism present in the brain (19). In this section, retrotransposition in the brain will be discussed, including some methods to study LINE-1 retrotransposition, cellular co-factors and the importance of LINE-1 retrotransposition in neurodegenerative diseases.

1.2.1 Proof of LINE-1 activity in the brain

In 2005, LINE-1 retrotransposition was proven for the first time in the nervous system. Muotri et al showed that LINE-1 retrotransposition occurred in rat hippocampal neuronal progenitor cells (NPCs) *in vitro* by making use of the LINE-1 retrotransposition assay (19). By utilising the same assay, LINE-1 retrotransposition was also demonstrated in human neuronal stem cells (20) and human NPCs derived from human fetal brain cells (21). The findings obtained *in vitro* were also validated *in vivo* using transgenic mice. The transgenic animals were generated by utilising a retrotransposition-competent human LINE-1 element that contained an enhanced green fluorescent protein (EGFP) reporter gene. Retrotransposition was observed with a quantitative polymerase chain reaction (qPCR) analysis using primers against the intron that interrupts the EGFP reporter gene. In these mice, LINE-1 insertions were obtained in neuronal tissues (19). LINE-1 insertions were not observed in other somatic tissues, like the heart (19).

The brain consists of many types of neuronal cells, such as NPCs and neurons. However, most neuronal cells do not divide. Therefore, it was important to examine whether retrotransposition also is found in nondividing neurons (22). Macia et al have shown that LINE-1 retrotransposition occurs in nondividing neuronal cells (23). Different neuronal cell types, such as NPCs and nondividing adult neuronal cells were tested for their capability of supporting LINE-1 retrotransposition. A higher number of LINE-1 copies was acquired for the nondividing adult neuronal cells compared to NPCs (23). It is now well established from a variety of studies that LINE-1 retrotransposition is occurring in differentiating neural stem cells, NPCs, differentiating neurons and nondividing neurons (18).

The LINE-1 retrotransposition assay does not allow the detection of endogenous levels of LINE-1 retrotransposition. Therefore, efforts were taken to investigate the endogenous levels of LINE-1 retrotransposition in the human brain. The endogenous levels were measured using a copy number variant (CNV) based *ex vivo* qPCR analysis on the genomic DNA of post-mortem human tissues (21). In contrast to the LINE-1 retrotransposition assay, transfection with an engineered human LINE-1 element was not performed. The genomic DNA was isolated from the tissues of interest and a qPCR was carried out with probes for the ORF2 gene. The analysis revealed a high content of the ORF2p in the hippocampus compared to other tissues, like the heart and the liver (21).

Baillie et al developed another method to detect endogenous levels of LINE-1 retrotransposition, namely the capture sequence protocol (24). By using this method, it was possible to map somatic LINE-1 insertions in post-mortem hippocampi and caudate nuclei. Based on their experiment, an irregular distribution of LINE-1 insertions was observed in the genes involved in neurogenesis and

synaptic function. These insertions are capable of creating genomic mosaicism and influencing neurobiological processes (24).

In the past, there was an interest in determining the number of complete LINE-1 insertions per neuron to check whether variation of the genome between single neurons in the brain occurs. Neurons from the cerebral cortex and caudate nucleus of 3 different individuals, were used by Evrony et al to perform single-neuron sequencing (25). They discovered in their experiment only 1.1 somatic LINE-1 insertions per neuron and less than 0.6 unique insertions (25). The obtained outcomes were in contrast to the hypothesis that LINE-1 retrotransposition contributes to neuronal diversity. As a remark, it should be noted that these results were never validated. Upton et al also attempted to determine the number of LINE-1 insertions and led to the surprising result of 13.7 somatic LINE-1 insertions per neuron present in the hippocampus (26). However, no further validation of the results occurred. To date, the exact extent of retrotransposition in the brain is still unknown (18).

1.2.2 Methods to explore LINE-1 retrotransposition

1.2.2.1 LINE-1 retrotransposition assay in cultured cells

The LINE-1 cell culture-based retrotransposition assay is a first method to detect LINE-1 retrotransposition. This assay makes it possible to gain insight into the process of retrotransposition and to study the role of cellular co-factors (27, 28).

Moran et al were the first to use this method to detect the competency of the LINE-1 reporter plasmid to retrotranspose in cultured cells (29). For this purpose, a retrotransposition indicator cassette, mNeoI, was introduced in the 3'-UTR of the LINE-1 plasmid. In this cassette, the selectable marker, here neomycin, is present in the antisense orientation with a heterologous promoter and a poly(A) signal (30). In the sense orientation, an intron is present that interrupts the selectable marker (29). The selectable marker can only be expressed when a full cycle of retrotransposition of the LINE-1 reporter plasmid occurs. First, the plasmid has to be transcribed, followed by splicing, resulting in removal of the intron. Subsequently, the spliced LINE-1 mRNA undergoes reverse transcription. As a result, a new LINE-1 copy is generated with the reporter gene in the opposite orientation. Next, this copy has to integrate into the sequence of the genomic DNA of the cultured cell. After the genomic DNA has been transcribed and translated, expression of the reporter gene can be detected. The expression of neomycin, the reporter gene, will only occur when a complete cycle of retrotransposition has taken place (27). To detect whether this complete cycle has occurred, cells are treated with G418, geneticin. The cells are only resistant to this antibiotic if they express the selectable marker (29).

A disadvantage of this construction is the antibiotic selection that is needed to determine retrotransposition. Ostertag et al designed a construct with an EGFP cassette instead of a neomycin reporter gene (31) (Fig. 1.3). The retrotransposition cassette consisted of the EGFP gene, a cytomegalovirus (CMV) immediate-early promoter in the 5' end, a poly(A) signal in the 3' end and a γ-globin intron in the antisense direction (31). Only after removal of the intron, the expression of EGFP can be detected. Retrotransposition events can be detected in two ways: flow cytometry and real-time quantitative polymerase chain reaction (RT-qPCR). Flow cytometry is applied to define the percentage of EGFP positive cells. The integrated copy number of the EGFP gene is estimated via RT-qPCR (32).
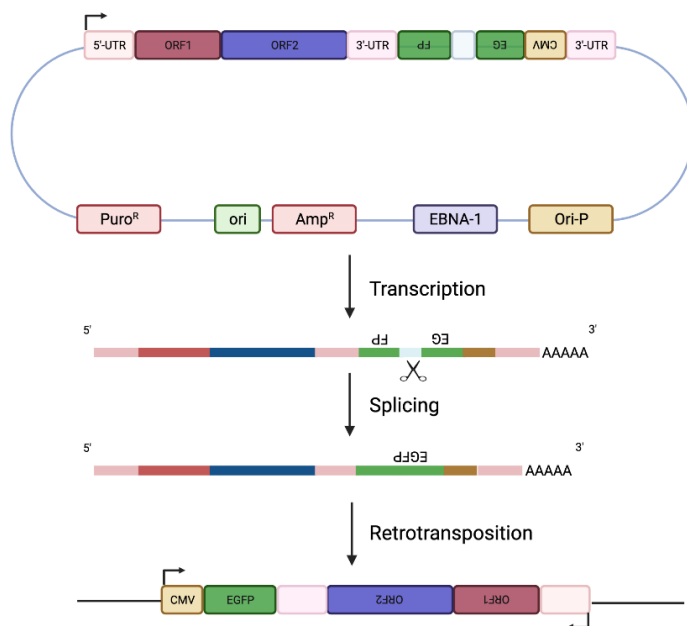

*Figure 1.3: LINE-1 reporter plasmid with the EGFP cassette. The LINE-1 reporter plasmid consists of a full-length LINE-1 element with in the 3'-UTR an EGFP reporter cassette orientated in the antisense direction. An γ-globin intron interrupts this reporter cassette. After transcription of this LINE-1 reporter plasmid, the intron is spliced. Next, retrotransposition takes place resulting in integration of the LINE-1 element in the genomic DNA. After transcription and translation of the genomic DNA, EGFP will be expressed. Replication in primate cells can occur due to the Epstein-Barr virus origin of replication (OriP) and the Epstein-Barr virus nuclear antigen 1 (EBNA-1). Resistance to ampicillin (AmpR) and E. Coli origin of replication (ori) allow replication in prokaryotic cells. Resistance to puromycin (PuroR) is used to select transfected cells. Figure adapted from: Rangwala et al, Methods, 2009, **49**(3), 219-226.*

1.2.2.2   Detecting endogenous LINE-1 retrotransposition

The LINE-1 cell culture-based retrotransposition assay only provides information that the cell supports LINE-1 retrotransposition. It does not tell how much endogenous LINE-1 activity is present in the cells since these cells are transfected with an engineered LINE-1 plasmid. There are other methods to detect the endogenous activity of LINE-1, such as a CNV based *ex vivo* qPCR assay and retrotransposon capture sequence protocol.

CNV based *ex vivo* qPCR assay. First, genomic DNA of the tissue of interest of which the endogenous LINE-1 activity needs to be determined, is isolated. Next, this extracted DNA is subjected to a qPCR assay with specific probes. Probes are used against the conserved 3' region of the ORF2p and a probe

against the 5'-UTR is used as a control (21). Since most of the LINE-1 insertions are truncated in their 5'-UTR, the copy number of the control is believed to be less in comparison to the probes against 3' region of the ORF2p (11).

Capture sequencing protocol. Capture sequencing enables the detection and localisation of endogenous LINE-1 insertions (33). The genomic DNA from the tissue of interest is isolated and genomic DNA of other tissue serves as control. In this method, Illumina libraries are improved with biotin-labelled probes targeting the 5'-UTR or 3'-UTR of LINE-1 (34). DNA parts labelled with these probes are captured by a dynabead-streptavidin (34, 35). Subsequently, captured DNA is obtained and further amplification and sequencing of this captured DNA are performed. This results in an amount of sequencing read with LINE-1 insertions in the genomic DNA. Afterwards, the data is observed *in silico* to search for known and unknown polymorphic insertions. All other insertions are unique to the tissue (34).

1.2.3   Regulation of LINE-1 retrotransposition

Since retrotransposition can affect cells in different ways, several responses to regulate LINE-1 activity have evolved. Several transcription factors are able to bind in the promoter region of LINE-1 due to the presence of binding sites (36). In addition, nuclear import of the LINE-1 RNP complex is a crucial step in the mechanism of LINE-1 retrotransposition. In this section the most important regulation systems will be mentioned.

1.2.3.1   Repression of LINE-1 activity

Several proteins have evolved the capacity to repress LINE-1 activity. From the sex determining region Y box (Sox) family, Sox2 is recognised to play a key role in the proliferation of neuronal stem cells and in keeping these neuronal stem cells multipotent (37). By binding on the LINE-1 promoter, Sox2 is responsible for the suppression of LINE-1 activity in these cells (19). The LINE-1 promoter consists of CpG dinucleotides, which are methylated in large numbers in neuronal cells. The methyl-CpG binding protein 2 (MeCP2) is mainly expressed in mature neurons and can bind to these methylated sites. The binding of MeCP2 to these methylated CpG dinucleotides leads to inhibition of LINE-1 activity (33, 38). Histone deacetylase 1 (HDAC1) is another known inhibitor of LINE-1 transcription (39). Another deacetylase, sirtuin 6 (SIRT6), is thought to inhibit LINE-1 activity by promoting the formation of heterochromatin (40). SIRT6 is localised on the LINE-1 promoter but becomes less common during ageing and oxidative stress (33). P53 is a crucial factor involved in the regulation of proliferation and

differentiation of neurons (41). It is known that P53 suppresses LINE-1 activity by playing a role in H3K9 trimethylation (42).

1.2.3.2 Enhancers of LINE-1 activity

When a neural stem cell starts with differentiation, the expression level of Sox2 is decreased, the LINE-1 promoter is demethylated and repressor complexes are dissociated from the LINE-1 (43). Simultaneously, Wnt3a stimulates the binding of a β-catenin activator complex to the transcription factor-lymphoid enhancer factor (TCF-LEF) binding site in the LINE-1 promoter region. The result is that an increased degree of LINE-1 retrotransposition is observed in NPCs (43). Ying-Yang factor 1 (YY1), a zinc finger protein transcription factor, facilitates LINE-1 transcription probably due to guiding the RNA polymerase II to its binding site (44). YY1 is expressed in large numbers in neurons and plays a role in neuronal differentiation (33). In the Sox family, another member Sox11 is specified as a transcriptional activator of LINE-1 (45). Committed neurons present in the neurogenic niche primarily express this protein (33). Runt-related transcription factor 3 (RUNX3) stimulates the LINE-1 promoter region and is concerned in development and survival of proprioceptive neurons and neurogenesis (33, 46).

1.2.3.3 The import of the LINE-1 RNP complex in the nucleus

The nuclear import of the LINE-1 RNP complex is an important step during retrotransposition. It is described that nuclear entrance of the LINE-1 RNP complex occurs during cell division (47). However, LINE-1 retrotransposition takes also place in nondividing cells, for example neurons (23). Nowadays, it is not yet clear how LINE-1 RNP complexes access in an independent manner of cell division the DNA of the host cell (48).

Transportin-1 (TNPO1) is one proposed host factor responsible for nuclear import of the LINE-1 RNP complex (48). TNPO1, also known as Karyopherin-β2 or Importin-β2, promotes the nuclear import of histone, ribosomal and viral proteins (49). The research group of Dr. I. Pedersen have shown that microRNA-128 (miRNA-128) is able to repress LINE-1 retrotransposition by directly binding to the LINE-1 ORF2 RNA or by downregulation of TNPO1 (48). This result suggests TNPO1 as a nuclear import factor of the LINE-1 RNP complexes. Besides TNPO1, transportin-3 (TNPO3 or TRN-SR2) is another member of the β-Karyopherin family. TNPO3 is renowned as a factor for nuclear import of serine/arginine-rich (SR) splicing factors (50, 51). SR proteins are identified as specific regulators and required factors during the splicing process of pre-mRNA (52). It is previously demonstrated that TNPO3 is the nuclear import factor of human immunodeficiency virus type 1 (HIV-1) (53). Interestingly, TNPO1 is recently discovered as a second nuclear import factor of HIV-1 (54).

To conclude, miRNA-128 is able to bind to mRNAs of all three transportins, but the role of the other transportins, besides TNPO1, in LINE-1 retrotransposition has not yet been studied (48).

1.2.4 LINE-1 retrotransposition and neurodegenerative diseases

Since LINE-1 insertions are present in the human brain, LINE-1 can contribute to the development of diseases (22). In this part, the focus will be on neurodegenerative diseases. Furthermore, the current status of the research on the link between LINE-1 and Parkinson's disease (PD) will be highlighted.

1.2.4.1 Ataxia-telangiectasia

Ataxia-telangiectasia (AT), a progressive neurodegenerative disorder is provoked by a mutation of the ataxia-telangiectasia mutated (ATM) gene (55). Patients with this disorder go through a dilation of their capillaries and a loss of motor function (36). Sometimes problems, such as acquired diabetes and immunodeficiency, are involved in this disease (36).

In the past, it was found that ATM has serine/threonine-protein kinase activity and detects double-strand breaks in DNA (56). Upon detection of this DNA damage, a signalling cascade is activated by phosphorylating its substrates, such as P53 (36). As a result, the cell cycle is arrested until the repair of these breaks (57). In cells that lack this ATM gene, DNA repair will not occur resulting in DNA mutagenesis increasing with the cell cycle (36). An increase in the ORF2 copy number and LINE-1 retrotransposition in neurons from AT patients was shown by Coufal et al (58). This observed increase prompts that ATM gene modulates LINE-1 retrotransposition activity.

1.2.4.2 Alzheimer's Disease

Another neurodegenerative disorder is Alzheimer's disease (AD), of which the link with LINE-1 was investigated. Patients experience progressive impairments in memory and cognitive ability. Patients with AD are diagnosed at the age of 65 and older (59). AD is characterised by an accumulation of extracellular amyloid plaques and the presence of intracellular neurofibrillary tangles of Tau protein in the affected brain regions (60).

The role of LINE-1 in patients with AD was investigated by Bollati et al by performing bisulfite-qPCR pyrosequencing on the brain tissue of these patients and healthy controls (61). Compared to the control group, LINE-1 activity was increased in these patients with AD (61). In contrast, Hernandez et al detected no difference in DNA methylation of LINE-1 when investigating peripheral blood samples of late-onset AD patients in comparison to healthy controls (62). Since it is known that DNA methylation of LINE-1 guides to suppression of LINE-1 activity, this study suggested no difference

between healthy controls and AD patients. There is a need to conduct further research to understand the direct link between LINE-1 methylation and the pathogenesis of AD.

1.2.4.3   Parkinson's Disease

Selective loss of dopaminergic neurons in midbrain substantia nigra causes PD, a neurodegenerative movement disorder (63). In particular, the ageing population is affected by this disorder and experiences bradykinesia, rest tremor and rigidity (64). Recently, several studies were conducted to define a link between LINE-1 and PD. In this section, the main findings of these studies will be highlighted.

A small-scale study observed a decrease in DNA methylation levels of patients with PD compared to healthy individuals (65). Since DNA methylation suppresses LINE-1 retrotransposition, it was hypothesised that more retrotransposition would occur in patients with PD. A new comparison of the DNA methylation levels between PD patients and healthy individuals was performed (63). Here, no difference was seen in the levels of DNA methylation between healthy persons and PD patients. One explanation for the different results could be that in the small-scale study only PD patients in an advanced stage of the disease were included. Therefore, DNA methylation levels may have been affected (63).

Another association between LINE-1 and PD is sought at the level of neurons. During the process of ageing, the mesencephalic dopaminergic (mDA) neurons lose their function (66). This dysfunction is accelerated by exposure to stressors, such as neurotoxins, resulting in the death of these neurons. As a consequence, a neurodegenerative disease, like PD, can develop (67). Two homeoprotein transcription factors, Engrailed-1 and Engrailed-2, are present in these mDA neurons. Moreover, Engrailed-2 has a protective role in situations of oxidative stress (68). A link between LINE-1, Engrailed and oxidative stress was investigated by the research group of Dr. A. Prochiantz (67). First, they noticed a higher level of LINE-1 activity in cultured mDA neurons when they were exposed to H_2O_2, an inducer of oxidative stress. The same increase in LINE-1 expression was observed in *in vivo* mDA neurons after exposure to 6-hydroxydopamine (67). Overexpression of LINE-1 increased the number of DNA strand breaks. Second, Engrailed was identified as a repression factor of LINE-1 activity. It can be suggested that the protective properties of Engrailed against DNA breaks induced by oxidative-stress, are partly through direct LINE-1 suppression (67). There exist several mouse models of PD, one of these models is the *En1*-het mouse where only one allele for Engrailed-1 is present. In this model, the mDA neurons were more sensitive to oxidative stress and their death was induced more quickly (67, 69). In addition, an upregulation of LINE-1 was observed in the substantia nigra of these mice (67).

Another commonly used model to study PD is Lund Human Mesenphalic (LUHMES) cells (70). These cells can be differentiated into dopaminergic neuronal cells and are often used to study neurodegeneration of these cells (70, 71). Administration of 1-methyl-4-phenylpyridinium (MPP+) and rotenone, two inhibitors of the mitochondrial respiratory chain complex I, have demonstrated a significant increase of the ORF1p in the nucleus. This result was validated by the administration of phenothiazine, a radical scavenger. Indeed, after the addition of phenothiazine, a decrease in the ORF1p was seen. The administration of 1-methyl-4-phenyl-1,2,3,6-tetrahydropyridine (MPTP), a precursor of MPP+, also resulted in an increase of the ORF1p in wild-type (WT) mice *in vivo* (72). The increase disappeared with phenothiazine (72).

In 2020, Pfaff et al have focused on RC-LINE-1s in the reference and non-reference genome of human individuals (73). The polymorphic nature of these RC-LINE-1s can contribute to neurological disease, emphasising the relevance to study the presence of these RC-LINE-1s in PD. A whole-genome sequencing experiment was conducted in healthy individuals and patients with PD from the Parkinson's Progression Markers Initiative. Pfaff et al focused on 16 highly active RC-LINE-1s and demonstrated that individuals with 9 or more of these highly active RC-LINE-1s have a higher risk to PD (73).

To date, several studies have tried to investigate the link between LINE-1 and PD. Despite the preliminary result of a small-case study, no difference was found in DNA methylation levels between PD patients and healthy individuals in a subsequent study. Further research in the context of Engrailed and LINE-1 will also have to show what the exact role of LINE-1 is in PD. Based on the results of the study on LUHMES cells, there is a possible link between LINE-1, PD and oxidative stress. Although it is demonstrated that individuals with 9 or more of highly active RC-LINE-1s have a higher risk to PD, further investigation is needed to examine the burden of LINE-1 activity on PD. Together these studies indicate a possible involvement of LINE-1 in PD.

1.3 REVERSE TRANSCRIPTASE INHIBITORS

A LINE-1 element contains an ORF2, which encodes the ORF2p with EN and RT activities. Since the RT is important during the TPRT of a LINE-1 element, several studies have explored the influence of RT inhibitors on LINE-1 retrotransposition.

In general, RT inhibitors can be classified into 3 different types: nucleoside analogue RT inhibitors (NRTIs), nucleotide analogue RT inhibitors (NtRTIs) and non-nucleoside RT inhibitors (NNRTIs) (74, 75). NRTIs and NtRTIs are competitive inhibitors for the native deoxynucleotide triphosphates during

reverse transcription (76). The lack of a 3'-OH causes them to act as chain terminators of DNA (74, 77). NNRTIs bind very specifically to an NNRTI pocket of the HIV-1 RT and have a different mechanism of action (78, 79). Their binding results in the inhibition of the enzyme in an allosteric, non-competitive manner (80).

Some RT inhibitors used in the treatment of HIV-1 have shown to inhibit LINE-1 retrotransposition in a dose-dependent manner (74, 81). Indeed, the use of RT inhibitors is well described in the literature. Azidothymidine and stavudine were able to inhibit LINE-1 retrotransposition at concentrations of 5 µM in a tissue culture retrotransposition assay (74). Recently, lamivudine and emtricitabine, both HIV-1 NRTIs, were also identified as inhibitors of LINE-1 (82). These were tested in the LINE-1 retrotransposition assay performed in HeLa cells and HEK293T cells. Different reporter genes, such as the neomycin phosphotransferase gene or the blasticidin S deaminase reporter gene, were used (82). Contradictory results are present in the literature when it comes to NNRTIs. It was reported that efavirenz was able to inhibit LINE-1 retrotransposition by 70 %, whereas nevirapine only gave a decrease of 10 % in LINE-1 retrotransposition (74). In contrast, efavirenz and nevirapine did not affect LINE-1 activity in the LINE-1 retrotransposition assay performed by the research group of Dr. J. L. Garcia-Perez (82). A possible explanation for the observed difference between the different research groups could be the use of different LINE-1 elements or LINE-1 retrotransposition assays.

Recently, RT inhibitors were used in a pilot clinical study to treat Aicardi-Goutières syndrome (AGS) (60). AGS is a neuroinflammatory disease, characterized by an upregulation of the type I interferon (IFN-1) production (60, 83). Mutations in three prime repair exonuclease 1 (TREX1) and SAM and HD domain-containing deoxynucleoside triphosphate triphosphohydrolase 1 (SAMHD1) genes are responsible for an AGS phenotype (60, 84, 85). Besides, it is known that both TREX1 and SAMHD1 suppress LINE-1 activity (60). It was hypothesised that in these patients an upregulation of LINE-1 would occur resulting in an upregulation of IFN-1. By inhibition of LINE-1 activity by anti-HIV RT therapy, a reduction in IFN-1 signalling was expected. Indeed, the results of the clinical study supported the hypothesis and a reduction in IFN-1 was observed (12).

To date, a crystal structure is not available of the RT domain of a LINE-1 element (82). This makes it hard to make binding predictions of the RT inhibitors (82). Once this crystal structure is available, more potent and specific inhibitors of the LINE-1 RT can be created.

2 OBJECTIVES

There is growing evidence that LINE-1 is acting as a possible pathogen in human diseases. However, not much is known about the host factors involved in LINE-1 retrotransposition. Therefore, new insights in the process of LINE-1 retrotransposition and the interactome of LINE-1 are needed. Recently, it was discovered that miRNA-128 downregulates TNPO1 resulting in a decrease in LINE-1 retrotransposition (48). The decrease in LINE-1 retrotransposition was also observed in TNPO1 KD HeLa cells created with a TNPO1-specific short hairpin RNA (shRNA) (48). This finding identifies TNPO1 as a potential nuclear import factor of the LINE-1 RNP complexes. The mRNA of TNPO3 is also targeted by miRNA-128, but the effect on LINE-1 retrotransposition has not yet been tested (48). Interestingly, TNPO1 was recently identified as a second nuclear import factor of HIV-1 (54). TNPO3 is a factor involved in the nuclear import of HIV-1 (53). The first objective of this master thesis is to identify transportins as host factors of LINE-1 retrotransposition. HEK293T TNPO1 and TNPO3 depleted cell lines will be created by a specific microRNA-30 (miRNA) targeting the mRNAs of TNPO1 and TNPO3. Depletion will be validated on Western Blot and RT-qPCR. Afterwards, the effect of TNPO1 and TNPO3 depletion will be tested in the LINE-1 retrotransposition assay.

The LINE-1 retrotransposition assay is optimized in HEK293T cells in the host lab. Since LINE-1 retrotransposition is present in the brain, contributes to mosaicism of the genome and is involved in the development of neurological disorders, it is relevant to optimize the LINE-1 retrotransposition assay in a neuronal cell line. The LINE-1 retrotransposition assay has been executed before in SK-N-BE(2)-C cells, a neuroblastoma derived cell line (32). These cells were able to support LINE-1 retrotransposition. The second objective of this master thesis is to optimize the LINE-1 retrotransposition assay in SH-SY5Y cells, another neuroblastoma derived cell line. Since SH-SY5Y cells are difficult to transfect, the transfection efficiency needs to be optimized first. Different approaches will be taken to optimize the transfection of SH-SY5Y cells.

An upregulation of LINE-1 activity has been reported in a Parkinson's disease murine model, namely *En1*-het mice (67). These mice are heterozygous for the allele of Engrailed-1, resulting in dopaminergic neurons that are more vulnerable to oxidative stress and die more quickly. In the dopaminergic neurons of the substantia nigra of these mice, an increase of LINE-1 expression was observed (67). To investigate the role of LINE-1 in other Parkinson's disease animal models, a method to detect the endogenous ORF1p expression is needed. The third objective of this master thesis is to optimize the immunohistochemical and immunofluorescent staining for the ORF1p on coronal brain slices of C57BL/6J WT mice.

3   MATERIALS AND METHODS

3.1   CELL CULTURE

HEK293T cells were cultured in Dulbecco's modified Eagle medium (DMEM) with GlutaMAX supplement (Gibco) supplemented with 5 % (v/v) fetal bovine serum (FBS; Gibco) and 0.005 % (w/v) gentamicin (Gibco). SH-SY5Y cells were cultured in DMEM with GlutaMAX supplement (Gibco) supplemented with 15 % (v/v) FBS (Gibco), 0.005 % (w/v) gentamicin (Gibco) and 1 % (v/v) MEM non-essential amino acids (Gibco). HEK293T and SH-SY5Y cells were grown at 37° C and 5 % CO_2. Both cell lines were tested on a regular basis to exclude mycoplasma contamination.

3.2   CLONING AND PLASMID CONSTRUCTS

For the viral vector production of TNPO1 and TNPO3 knock-down (KD) cells, transfer plasmids which encode a miRNA-based shRNA were already available in the host lab. Five different DNA sequences encoding a TNPO1-specific miRNA-based shRNA were cloned into a pGAE backbone containing a blasticidin resistance gene (BsdR) and a woodchuck hepatitis virus post-transcriptional regulatory element (WPRE) (Table 3.1). The miRNA is driven by a spleen focus forming virus (SFFV) promoter. Three different DNA sequences encoding a TNPO3-specific miRNA-based shRNA were cloned in the same pGAE backbone as described for TNPO1 (Table 3.1).

To perform the LINE-1 retrotransposition assay the 99-L1RPS-EGFP-Puro (L1RP) plasmid consisting of an active L1RP retrotransposon and the 99-JM111-EGFP-Puro (JM111) control plasmid containing 2 missense mutations in the L1RP retrotransposon were used. Prof. T. Gramberg, from Friedrich-Alexander-University (located in Erlangen-Nürnberg Germany), generously gave previously mentioned plasmids (31). The L1RP element is driven by its native promoter. The EGFP retrotransposition cassette driven by the CMV promoter is present in both plasmids. To determine transfection efficiency in SH-SY5Y cells, a green fluorescent protein (GFP) mock reporter plasmid of 6 kb was used. An 18 kb plasmid containing the leucine-rich repeat kinase 2 (LRRK2) gene fused to the EGFP gene as described in (86), was also used to determine transfection efficiency. Both plasmids were available in the host lab.

Table 3.1: Overview of used specific miRNA-based shRNA

miRNA	Sequence	Targeting
TNPO1_miRNA-1	AAGAAGGTATATTGCTGTTGACAGTGAGCGGCGTACTGTGAACCTGT GTATTTAGTGAAGCCACAGATGTAAATACACAGGTTCACAGTACGGT GCCTACTGCCTCGGACTTCAAGGG	CDS
TNPO1_miRNA-2	AAGAAGGTATATTGCTGTTGACAGTGAGCGCCTCTAATGTTGCACAT TGATTTAGTGAAGCCACAGATGTAAATCAATGTGCAACATTAGAGCT GCCTACTGCCTCGGACTTCAAGGG	CDS
TNPO1_miRNA-3	AAGAAGGTATATTGCTGTTGACAGTGAGCGTGTACTCAGACATAGAT ATTATTAGTGAAGCCACAGATGTAATAATATCTATGTCTGAGTACTTG CCTACTGCCTCGGACTTCAAGGG	CDS
TNPO1_miRNA-4	AAGAAGGTATATTGCTGTTGACAGTGAGCGAGCCGTTGCATCATGGA TTAACTAGTGAAGCCACAGATGTAGTTAATCCATGATGCAACGGCATG CCTACTGCCTCGGACTTCAAGGG	CDS
TNPO1_miRNA-5	AAGAAGGTATATTGCTGTTGACAGTGAGCGTCAATTCTATAGCGCACA ATAATAGTGAAGCCACAGATGTATTATTGTGCGCTATAGAATTGTTGC CTACTGCCTCGGACTTCAAGGG	5'-UTR
TNPO3_miRNA-1	AAGAAGGTATATTGCTGTTGACAGTGAGCGGCCGATTACCTTTGGATA AGATTAGTGAAGCCACAGATGTAATCTTATCCAAAGGTAATCGGGTGC CTACTGCCTCGGACTTCAAGGG	CDS
TNPO3_miRNA-2	AAGAAGGTATATTGCTGTTGACAGTGAGCGACGGCGCACAGAAATTA TAGAATAGTGAAGCCACAGATGTATTCTATAATTTCTGTGCGCCGATG CCTACTGCCTCGGACTTCAAGGG	CDS
TNPO3_miRNA-3	AAGAAGGTATATTGCTGTTGACAGTGAGCGTCCAGACTGTGTCCCACA ATCATAGTGAAGCCACAGATGTATGATTGTGGGACACAGTCTGGTTGC CTACTGCCTCGGACTTCAAGGG	5'-UTR

CDS: coding sequence; UTR: untranslated region.

3.3   LENTIVIRAL VECTOR PRODUCTION

Simian immunodeficiency virus (SIV) vector production was performed using branched polyethyleneimine (in-house) as a transfection reagent. 24 h before transfection 6×10^6 HEK293T cells were seeded in a 10 cm dish in DMEM with GlutaMAX supplement (Gibco) supplemented with 2 % (v/v) FBS (Gibco). Before triple transfection, the medium was changed with Opti-MEM (Gibco). HEK293T cells were transfected with 5 µg of the envelope plasmid VSV-G, 15 µg of the packaging plasmid SIV ENV and 15 µg of the transfer vector plasmid pGAE for SIV vector production. 24 h after transfection, the medium was changed by DMEM with GlutaMAX supplement (Gibco) supplemented with 2 % (v/v) FBS (Gibco). After 48 and 72 h, the medium was collected and filtered over a 0.45 µm Millex-GS Syringe Filter Unit (Merck Millipore). The obtained vector was concentrated with an Amicon® Ultra-15 Centrifugal Filter Unit (Merck Millipore) and stored at -80°C.

3.4   PRODUCTION OF KNOCK-DOWN CELL LINES

2×10^4 HEK293T cells/well were seeded in a 96-well plate 24 h before transduction. To generate stable TNPO1 KD and TNPO3 KD HEK293T cell lines, cells were transduced with a serial dilution of the appropriate viral vector in DMEM with GlutaMAX supplement (Gibco) supplemented with 8 % (v/v) FBS (Gibco) and 0.005 % (w/v) gentamicin (Gibco). After transduction, cells were kept under selection with 0.0005 % (w/v) blasticidin (Invivogen). Western Blot and RT-qPCR were performed to validate KD.

A scrambled control HEK293T cell line was already available in the host lab and was generated by transduction with a viral vector encoding a non-targeting miRNA-based shRNA. Cells were kept under selection with 0.0005 % (w/v) blasticidin (Invivogen).

3.5   GENERATION OF MONOCLONAL CELL LINES

From the polyclonal TNPO1 KD and TNPO3 KD HEK293T cells, a monoclonal cell line was generated. Cells were seeded at a density of 0.5 cells/well in a 96-well plate in medium consisting of DMEM with GlutaMAX supplement (Gibco) supplemented with 10 % (v/v) FBS (Gibco) and DMEM with GlutaMAX supplement (Gibco) supplemented with 5 % (v/v) FBS (Gibco), 0.005 % (w/v) gentamicin (Gibco) and 0.0005 % (w/v) blasticidin (Invivogen). After 1 week, wells were checked for the presence of a single colony. Monoclonal cells were continuously kept under selection with 0.0005 % (w/v) blasticidin (Invivogen). KD of TNPO1 or TNPO3 in monoclonal cell lines was validated on Western Blot and/or RT-qPCR.

3.6   DETERMINATION OF GROWTH CURVE

To determine the growth curve of various HEK293T-derived cell lines, 2.5×10^4 cells/well were seeded in a 24-well plate in the appropriate growth medium. After 24, 48, 72 and 96 h in culture, cells were trypsinized and counted with the TC20™ Automated Cell Counter (Bio-Rad).

3.7   WESTERN BLOT ANALYSIS

2×10^6 cells were collected and washed twice with phosphate buffered saline solution (PBS; Sigma-Aldrich®) followed by lysis with 1 % (w/v) sodium dodecyl sulfate (SDS; Acros Organics) buffer containing complete protease inhibitors cocktail, EDTA free (Sigma-Aldrich). Lysed samples were kept on ice for 30 minutes. Afterwards, samples were boiled for 10 minutes and passed multiple times

through a BD Micro-Fine syringe needle (BD Biosciences) to reduce viscosity. The BCA protein assay kit (Thermo Fisher Scientific) was used to determine the total protein concentration of the whole-cell lysate. Samples were loaded on a 4–15 % Criterion™ TGX™ Precast Midi Protein Gel (Bio-Rad) or an in-house 12.5 % SDS-polyacrylamide gel. After transfer to a nitrocellulose blotting membrane (GE Healthcare Life Sciences), the membrane was stained with Ponceau S solution (Sigma-Aldrich®) to check equal loading of the samples. 5 % (w/v) milk powder and PBS with 0.1 % (v/v) Triton-X100 (Acros Organics) was used to block the membrane. Subsequently, the membrane was incubated with primary antibody overnight at 4°C in blocking buffer. Mouse monoclonal anti-human TNPO1 (Santa Cruz Biotechnology) was used at 1/1000, rabbit monoclonal anti-human TNPO3 (Abcam) was used at 1/1000 and rabbit monoclonal anti-human LINE-1 ORF1p (Abcam) was used at 1/1000. Rabbit polyclonal anti-human glyceraldehyde 3-phosphate dehydrogenase (GAPDH; Abcam) at 1/1000 or mouse monoclonal anti-human vinculin (Sigma-Aldrich®) at 1/10000 was used to determine equal loading. Horseradish peroxidase-conjugated secondary antibodies anti-rabbit (Dako; 1/20000) and anti-mouse (Dako; 1/20000) IgG were used for detection by chemiluminescence with Clarity Western ECL substrate (Bio-Rad). For detection, an Amersham ImageQuant 800 biomolecular imager (GE Healthcare Life Sciences) was used.

3.8   RT-QPCR

To determine expression on mRNA levels, RT-qPCR was performed. Total RNA was extracted with the Aurum Total RNA Mini Kit (Bio-Rad). Spectrophotometric analysis with the Nanophotometer (Implen) was performed to determine the RNA concentrations. A total amount of 5 µg RNA was used to perform reverse transcription with the High-capacity cDNA Archive Kit (Applied Biosystems). LightCycler 480 SYBR Green I Master (Roche) or TaqMan-probes with IQ-Supermix (Bio-Rad) was used to perform RT-qPCR with the LightCycler480 (Roche) as detection system. Primers for β-actin were used to normalize the mRNA levels. The specific primers used in RT-qPCR are listed in Table 3.2.

To determine the integrated copy number of the LINE-1 EGFP element, genomic DNA was isolated at day 13 post-transfection with the Mammalian Genomic DNA miniprep kit (Sigma-Aldrich®). Spectrophotometric analysis with the Nanophotometer (Implen) was performed to determine the DNA concentrations. RT-qPCR analysis was performed with the LightCycler 480 SYBR Green I Master (Roche). The LightCycler 480 (Roche) or the CFX96 Touch Deep Well Real-Time PCR System (Bio-Rad) was used as detection system. Primers flanking the γ-globin intron were used to determine retrotransposition (Table 3.2). Primers for genomic β-actin were used to normalize the DNA levels (Table 3.2).

Table 3.2: Overview of primers used during RT-qPCR

Primers for RT-qPCR	Sequence
Copy DNA	
β-actin_Forward	CAC TGA GCG AGG CTA CAG CTT
β-actin_Reverse	TTG ATG TCG CGC ACG ATT T
TNPO1_Forward	CCC TGG ATG TTC TTG CAA AT
TNPO1_Reverse	AGC ATG TTA TGG AAC GCA CA
TNPO3_Forward	CTA CCA GAT GTG GCT GAA GT
TNPO3_Reverse	ACA AAA AGT CGG TCT GTC AA
Genomic DNA	
β-actin_Forward	TCA CCC ACA CTG TGC CCA TCT ACG A
β-actin_Reverse	CAG CGG AAC CGC TCA TTG CCA ATG G
LINE-1_EGFP_Forward (32)	GGTCACGAACTCCAGCAG
LINE-1_EGFP_Reverse (32)	CAGAAGAACGGCATCAAGG

3.9   LINE-1 RETROTRANSPOSITION ASSAY

HEK293T cells were seeded at a density of 5 x 10^4 cells/well in a 48-well plate in DMEM with GlutaMAX supplement (Gibco) supplemented with 10 % (v/v) FBS (Gibco) and 0.005 % (w/v) gentamicin (Gibco) prior to transfection. Transfection with the L1RP or the JM111 plasmid was carried out with FuGENE6 (Promega). The transfection mix consisting of 1 µg of DNA in 50 µL Opti-MEM (Gibco) and 4.5 µL FuGENE6 (Promega) in 50 µL Opti-MEM (Gibco) was incubated for 20 minutes at room temperature. To each well, 12 µL of the transfection mix and 120 µL of Opti-MEM (Gibco) was added. Non-transfected wells were used as a negative control. After 24 h, transfection was stopped by replacing the medium by DMEM with GlutaMAX supplement (Gibco) supplemented with 10 % (v/v) FBS (Gibco) and 0.005 % (w/v) gentamicin (Gibco). Cells were transferred to a 12-well plate 48 h post-transfection and selection with 0.00002 % (w/v) puromycin (Invivogen) was started from 72 h post-transfection onwards. On day 6 post-transfection, cells were transferred to a 6-well plate. Samples for flow cytometry were taken on day 6, 10 and 13 post-transfection.

SH-SY5Y cells were seeded at a density of 3.5 x 10^4 or 5.0 x 10^4 cells/well in a 48-well or 24-well plate, respectively, in DMEM with GlutaMAX supplement (Gibco) supplemented with 15 % (v/v) FBS (Gibco), 0.005 % (w/v) gentamicin (Gibco) and 1 % (v/v) MEM non-essential amino acids (Gibco). Co-transfection of the L1RP plasmid or the JM111 plasmid with a GFP mock reporter plasmid was

carried out using different transfection reagents (FuGENE6 (Promega), LipofectamineLTX (Invitrogen) and Lipofectamine3000 (Invitrogen)). The protocol as described above for the HEK293T cells was followed for FuGENE6, while the protocol of the manufacturer was followed for LipofectamineLTX and Lipofectamine3000. The used amount of DNA for the co-transfection per condition is listed in Table 3.3. After 24 h, transfection was stopped by changing the medium. Samples to determine transfection efficiency were taken 48 h post-transfection. To determine the transfection efficiency of the larger LRRK2-EGFP plasmid, 2×10^5 SH-SY5Y cells/well were seeded in a 24-well plate. Cells were co-transfected with the L1RP and a GFP mock reporter plasmid or were transfected with the LRRK2-EGFP plasmid using Lipofectamine3000. The used amount of DNA per condition is listed in Table 3.3.

Table 3.3: Used amount of DNA for co-transfection/transfection in SH-SY5Y cells

	48-well plate			24-well plate
Transfection reagent	*FuGENE6*	*LipofectamineLTX*	*Lipofectamine3000*	
DNA (µg)				
L1RP	1	0.750	0.300	0.500
JM111	-	-	-	0.500
GFP mock	0.500	0.375	0.150	0.250
LRRK2-EGFP	-	-	-	0.500

The full LINE-1 retrotransposition assay in SH-SY5Y cells with FuGENE6 was performed by following the protocol as described above for the HEK293T cells, except cells were plated in their appropriate growth medium and kept in a 48-well plate. Samples for flow cytometry were taken on day 6, 9, 13, 16 and 20 post-transfection. The full assay with Lipofectamine3000 was performed according to the protocol of the manufacturer. For this experiment, 1×10^5 cells/well were seeded in a 24-well plate.

Nucleofection of SH-SY5Y cells with the pmaxGFP® vector (Lonza) or the LRRK2-EGFP plasmid was carried out following the protocol of the manufacturer. The Cell Line Nucleofector™ Kit V (Lonza) was used with the A-023 program of the Nucleofector™ I Device (Lonza). Different plating densities were tested. For the LRRK2-EGFP plasmid, a DNA amount of 2, 4 or 6 µg was tested.

3.10 FLOW CYTOMETRY

Samples taken for flow cytometry were immediately fixed by adding 1:1 of 4 % (v/v) paraformaldehyde. The percentage of GFP or EGFP positive cells and the median fluorescence intensity (MFI) were measured with the Guava EasyCyte flow cytometer (Luminex). Living population was determined by the side scatter versus forward scatter profile. Data were analysed using the GuavaSoft 3.1 InCyte software packet provided by the instrument.

3.11 HISTOLOGY

Coronal brain slices of C57BL/6J WT mice were stored in 0.1 % (w/v) sodium azide in PBS as floating sections at 4°C. Before performing immunohistochemistry or immunofluorescence, floating sections were washed in PBS and antigen retrieval with 0.1 M citrate buffer of pH 6 was performed.

For immunohistochemistry, floating sections were treated with 3 % (v/v) H_2O_2 and 10 % (v/v) methanol in PBS to quench endogenous peroxidase activity. Sections were incubated with primary antibody in 0.1 % (v/v) Triton-X100 (Acros organics) in PBS solution with 10 % (v/v) goat serum (Dako) overnight at room temperature. The rabbit monoclonal anti-mouse LINE-1 ORF1p antibody (Abcam) was used in a dilution of 1/100. Goat biotinylated anti-rabbit IgG (Dako) was used as secondary antibody in a dilution of 1/600. The streptavidin-horseradish peroxidase complex (Dako; 1/1000) was added for incubation of the floating sections. The LINE-1 ORF1p was visualized using 3,3-diaminobenzidine (DAB; Sigma-Aldrich) as chromogen. Sections were rinsed and dehydrated before being mounted with coverslips using DPX mounting medium (Sigma-Aldrich®).

For immunofluorescence, floating sections were blocked with 0.1 % (v/v) Triton-X100 (Acros organics) in PBS with 10 % (v/v) goat serum (Dako). Sections were incubated with primary antibody in 0.1 % (v/v) Triton-X100 (Acros organics) in PBS solution with 10 % (v/v) goat serum (Dako) overnight at room temperature. For double staining, the rabbit monoclonal anti-mouse LINE-1 ORF1p antibody (Abcam) was used in a dilution of 1/100 and the chicken monoclonal anti-mouse tyrosine hydroxylase (TH; Aves Labs) was used in a dilution of 1/1000. Sections were incubated with fluorochrome-conjugated goat anti-rabbit Alexa 488 (Dako) or anti-chicken Alexa 555 (Dako) IgG in a dilution of 1/500 in the dark. After being rinsed, sections were covered with Mowiol (Sigma-Aldrich®) and DAPI (1/500; Invitrogen).

3.12 STATISTICAL ANALYSIS

The GraphPad Prism 9.1.0 software package and Excel were used for statistical analysis. Results are expressed as means ± standard deviation (SD) of technical replicates or independent biological replicates.

4 RESULTS

4.1 ROLE OF TNPO1 AND TNPO3 IN LINE-1 RETROTRANSPOSITION

4.1.1 Validation of polyclonal TNPO1 KD and TNPO3 KD cell lines

Polyclonal TNPO1 KD HEK293T cell lines were created by transduction of WT HEK293T cells with five different SIV vectors expressing a TNPO1-specific miRNA-based shRNA. To determine which miRNA gave the strongest KD, samples were taken to perform a RT-qPCR and Western Blot analysis. RT-qPCR revealed a strong KD of 79.5 % for the cell line created with TNPO1-miRNA-2 (Figure 4.1A). A Western Blot revealed no large difference in protein levels of TNPO1 in the created KD cell lines compared to the WT HEK293T cells (Figure 4.1B). Different amounts of protein were loaded for WT HEK293T cells to determine the linearity of the anti-TNPO1 antibody detection.
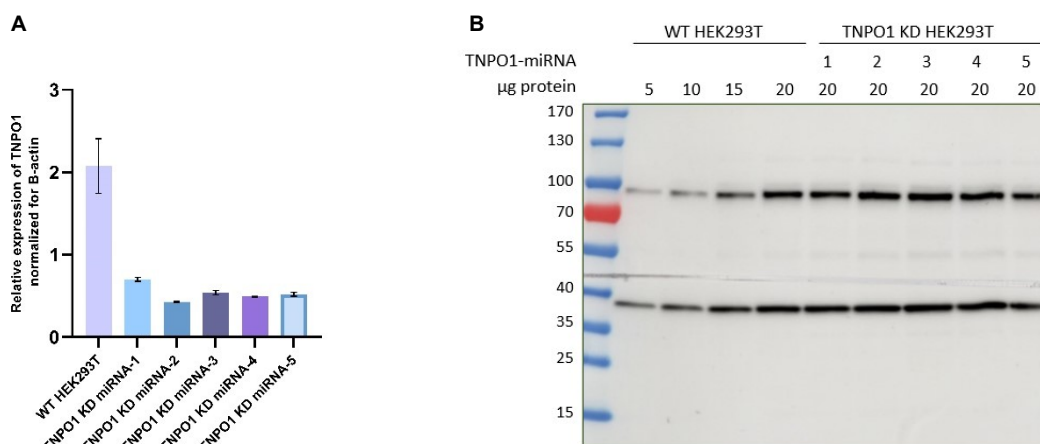

Figure 4.1: Validation of TNPO1 KD in HEK293T cells. A. Relative expression of TNPO1 normalized for β-actin in RT-qPCR. The TNPO1 mRNA level normalized for the β-actin mRNA level was determined in RT-qPCR. The strongest KD was corroborated in the cell line created with TNPO1-miRNA-2. The analysis was performed in technical triplicate and error bars represent the SD. B. Expression of TNPO1 and GAPDH on Western Blot. 5, 10, 15 and 20 μg of protein was loaded for WT HEK293T cells and 20 μg of protein was loaded for the TNPO1 KD cell lines. GAPDH was used as a loading control and gives a band at a height of 37 kDa. TNPO1 gives a band at a height of 96 kDa. The Western Blot did not reveal a strong KD on the protein level of TNPO1.

Similarly, three different SIV vectors expressing a TNPO3-specific miRNA-based shRNA were used to transduce WT HEK293T cells, resulting in polyclonal TNPO3 KD HEK293T cell lines. Samples of the three different polyclonal cell lines were taken to validate KD in RT-qPCR and Western Blot analysis. RT-qPCR revealed a KD of 84 % for the cell line created with TNPO3-miRNA-2 (Figure 4.2A). The KD of TNPO3 on protein level was visible on Western Blot and also revealed the strongest KD in the cell line created

with TNPO3-miRNA-2 (Figure 4.2B). For WT HEK293T cells, different amounts of protein were loaded to determine the linearity of the anti-TNPO3 antibody detection.
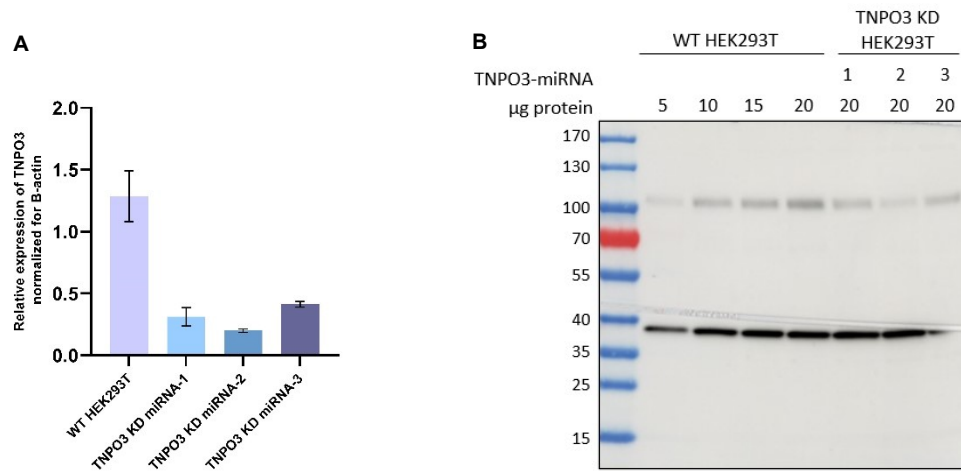

Figure 4.2: Validation of TNPO3 KD in HEK293T cells. A. Relative expression of TNPO3 normalized for β-actin in RT-qPCR. *The TNPO3 mRNA level normalized for the β-actin mRNA level was determined in RT-qPCR. The strongest KD was corroborated in the cell line created with TNPO3-miRNA-2. The analysis was performed in technical triplicate and error bars represent the SD.* ***B. Expression of TNPO3 and GAPDH on Western Blot.*** *5, 10, 15 and 20 μg of protein was loaded for WT HEK293T cells and 20 μg of protein was loaded for the TNPO3 KD cells. GAPDH was used as a loading control and gives a band at a height of 37 kDa. TNPO3 gives a band at a height of 105 kDa. Western Blot revealed the strongest KD in the cell line created with TNPO3-miRNA-2.*

4.1.2 Validation of monoclonal TNPO1 KD and TNPO3 KD cell lines

To obtain a clone with a strong KD, a monoclonal cell line was created starting from the polyclonal TNPO1 KD miRNA-4 and TNPO3 KD miRNA-2 cell line. First, the KD of these polyclonal cell lines was validated on Western Blot and RT-qPCR. The polyclonal TNPO1 KD miRNA-4 cell line, hereafter referred to as the polyclonal TNPO1 KD cell line, revealed a KD of 45 % on RT-qPCR and a KD of 38 % of the TNPO1 protein on Western Blot (Figure 4.3A-B). The polyclonal TNPO3 KD miRNA-2 cell line, hereafter referred to as the polyclonal TNPO3 KD cell line, corroborated a KD of 59 % in RT-qPCR and a KD of 91 % of the TNPO3 protein on Western Blot (Figure 4.3C-D). For both polyclonal cell lines, the percentage of KD decreased over time. Since a heterogeneous population of cells was present in cell culture, the cells with the stronger KD could be overgrown by cells with a lower KD. Therefore, the polyclonal cell lines were seeded at a density of 0.5 cells/well and single colonies were picked.

From the polyclonal TNPO1 KD cell line, 12 different clones were validated for their KD of TNPO1 in RT-qPCR (Figure 4.4A). The expression level of TNPO1 on mRNA level was determined for the polyclonal TNPO1 KD cell line and the derived monoclonal cell lines. The strongest KD was obtained for clones 9, 14, 15 and 16 with respectively a KD of TNPO1 of 62 %, 53 %, 65 % and 48 % (Figure 4.4A).

The polyclonal TNPO1 KD cell line gave a KD of 47 % (Figure 4.4A). These 4 colonies, which gave the strongest KD on RT-qPCR, were also validated on Western Blot (Figure 4.4B). Here, a KD of TNPO1 on protein level was observed in clones 14, 15 and 16 (Figure 4.4B).
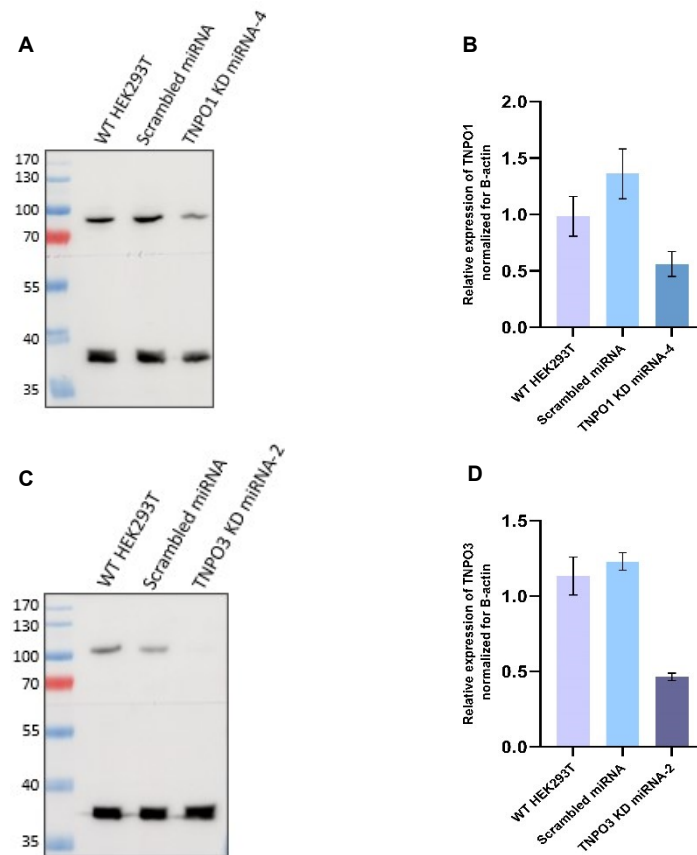

Figure 4.3: Validation of polyclonal KD cells on Western Blot and in RT-qPCR. A. Expression of TNPO1 and GAPDH on Western Blot. *10 µg of protein was loaded. GAPDH was used as a loading control and gives a band at a height of 37 kDa. TNPO1 gives a band at a height of 96 kDa and a KD of TNPO1 is visible in the TNPO1 KD miRNA-4 polyclonal cell line.* ***B. Relative expression of TNPO1 normalized for β-actin in RT-qPCR.*** *A KD of TNPO1 was corroborated in the TNPO1 KD miRNA-4 polyclonal cell line. Analysis was performed in technical triplicate and error bars represent the SD.* ***C. Expression of TNPO3 and GAPDH on Western Blot.*** *20 µg of protein was loaded. GAPDH was used as a loading control and gives a band at a height of 37 kDa. TNPO3 gives a band at a height of 105 kDa and a KD of TNPO3 is visible in the TNPO3 KD miRNA-2 polyclonal cell line.* ***D. Relative expression of TNPO3 normalized for β-actin in RT-qPCR.*** *A KD of TNPO3 was corroborated in the TNPO3 KD miRNA-2 polyclonal cell line. Analysis was performed in technical triplicate and error bars represent the SD.*

RT-qPCR was performed to validate the KD of 12 different clones resulting from the polyclonal TNPO3 KD cell line (Figure 4.4C-D). For both the polyclonal TNPO3 KD cell line and the derived monoclonal cell lines, the expression level of TNPO3 on mRNA level was determined. The strongest KD was obtained for clones 1, 6, 11, 14, 15 and 20 with respectively a KD of 55, 75, 52, 73, 69 and 57 % (Figure 4.4C-D). The polyclonal TNPO3 KD cell line gave a KD of 49 % of TNPO3 on the mRNA level (Figure 4.4C-D). The

KD of these 6 clones was also validated on the protein level of TNPO3 on Western Blot (Figure 4.4E). Here, the strongest KD was seen for clone 1, 6 and 11.
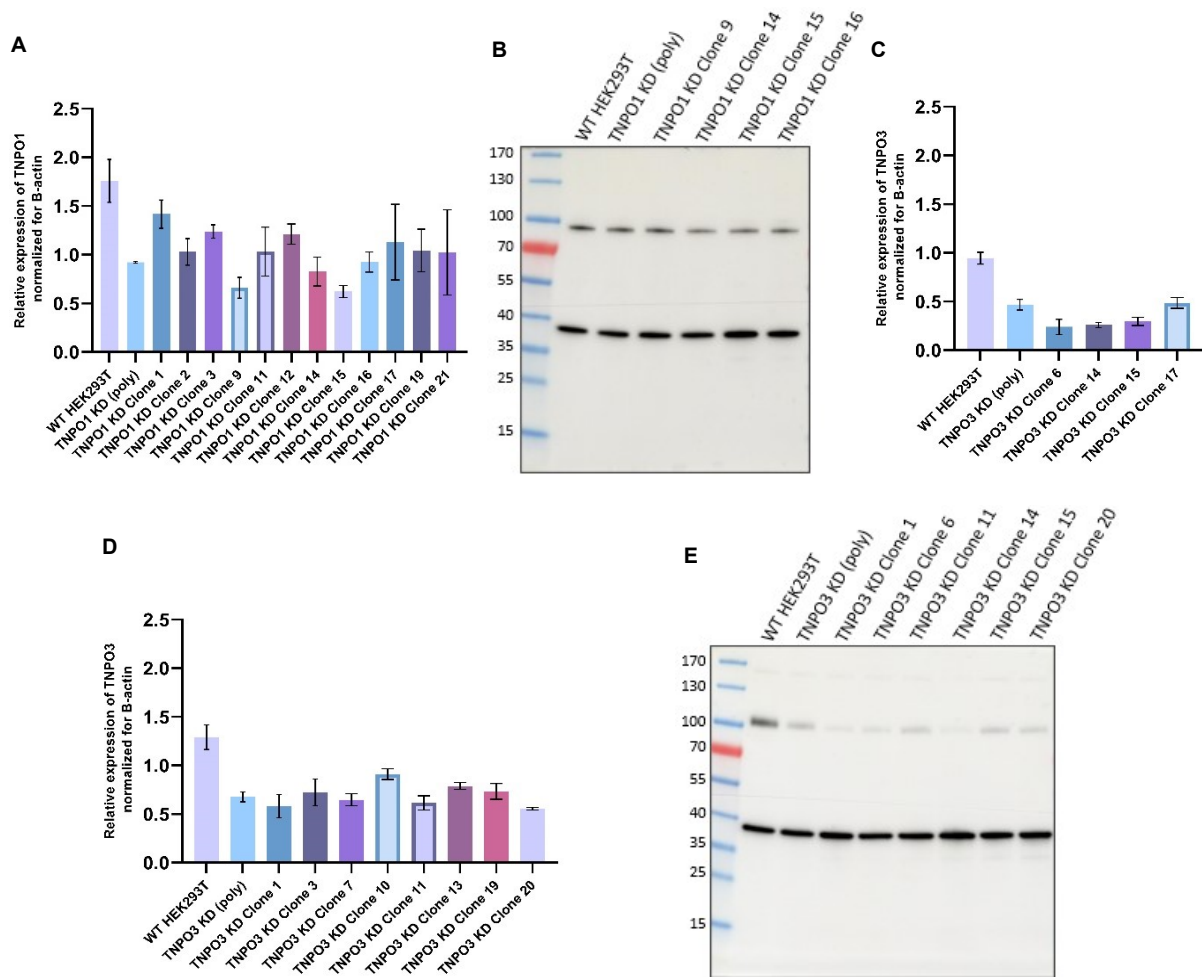

Figure 4.4: Validation of monoclonal cell lines. A. Relative expression of TNPO1 normalized for β-actin in RT-qPCR. *The mRNA level of TNPO1 was determined for the WT HEK293T cell line, polyclonal TNPO1 KD cell line and different monoclonal TNPO1 KD cell lines. The mRNA level of TNPO1 was normalized for the mRNA level of β-actin. The strongest KD of TNPO1 was corroborated in clone 9, 14, 15 and 16. Analysis was performed in technical duplicate and error bars represent the SD.* **B. Expression of TNPO1 and GAPDH on Western Blot.** *5 μg of protein was loaded. GAPDH was used as a loading control and gives a band at a height of 37 kDa. TNPO1 gives a band at a height of 96 kDa. The strongest KD on the protein level of TNPO1 was observed for clone 14, 15 and 16.* **C. & D. Relative expression of TNPO3 normalized for β-actin in RT-qPCR.** *The mRNA level of TNPO3 was determined for the WT HEK293T cell line, polyclonal TNPO3 KD cell line and different monoclonal TNPO3 KD cell lines. The mRNA level of TNPO3 was normalized for the mRNA level of β-actin. The strongest KD of TNPO3 was obtained in clone 1, 6, 11, 14, 15 and 20. Analysis was performed in technical triplicate and error bars represent the SD.* **E. Expression of TNPO3 and GAPDH on Western Blot.** *20 μg of protein was loaded. GAPDH was used as a loading control and gives a band at a height of 37 kDa. TNPO3 gives a band at a height of 105 kDa. The strongest KD on the protein level of TNPO3 was observed for clone 1, 6 and 14.*

4.1.3 Growth curves of various HEK293T-derived cell lines

During a transfection experiment, cell proliferation and viability play a crucial role in transfection efficiency. In the LINE-1 retrotransposition assay, the cell viability of the different cell lines can be considered as a key factor. The growth curve of the different HEK293T cell lines was determined to investigate the effect of the miRNA-based shRNA on cell proliferation. WT HEK293T, polyclonal TNPO1 KD, monoclonal TNPO1 KD (clone 15), polyclonal TNPO3 KD and monoclonal TNPO3 KD (clone 6) cells were plated in a 24-well plate and the number of cells per well was counted after 24, 48, 72 and 96 h (Figure 4.5). After logarithmic transformation of the data, simple linear regression revealed a non-significant difference between the slopes of the obtained growth curves.
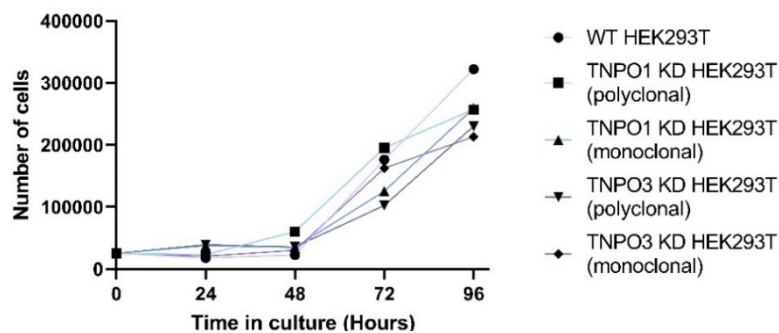

Figure 4.5: Growth curve of various HEK293T-derived cells. *The WT HEK293T, polyclonal TNPO1 KD, monoclonal TNPO1 KD (clone 15), polyclonal TNPO3 KD and monoclonal TNPO3 KD (clone 6) cell lines were seeded at a density of 2.5×10^4 cells/well in a 24-well plate. After 24, 48, 72 and 96 h in culture, cells were trypsinized and counted. Logarithmic transformation of the obtained data was performed (data not shown). Simple linear regression on the transformed data revealed a non-significant difference between the slopes of the different cell lines.*

4.1.4 TNPO1 and TNPO3 KD HEK293T cell lines in the LINE-1 assay

The LINE-1 retrotransposition assay allows investigating the role of TNPO1 and TNPO3 in LINE-1 activity. In the first experiment, the polyclonal TNPO3 KD miRNA-2 and TNPO3 KD miRNA-3 cell lines were tested. Together with the WT HEK293T cell line, these cells were plated in a 48-well plate at a density of 5×10^4 cells/well. FuGENE6 was used as a transfection reagent and cells were transfected with either the L1RP plasmid or the JM111 plasmid as a negative control. From day 3 post-transfection, puromycin was added to select the transfected cells. On day 6 and 13 post-transfection, samples for flow cytometry were taken. On day 13 post-transfection, samples for genomic DNA extraction were also taken. Flow cytometry analysis revealed a significant decrease in LINE-1 retrotransposition in polyclonal TNPO3 KD miRNA-3 cells on day 6 and 13, but a non-significant decrease in polyclonal TNPO3 KD miRNA-2 cells (Figure 4.6A). The relative integrated copy number of the LINE-1 EGFP element, using primers flanking the γ-globin intron, was determined with RT-qPCR. When the LINE-1

EGFP element is spliced, a product of 206 bp is amplified with RT-qPCR (32). In contrast, if the cassette is not spliced, the product of 1109 bp is not amplified with RT-qPCR (32). A significant decrease in relative integrated copy number was observed in polyclonal TNPO3 KD miRNA-3 cells compared to WT HEK293T cells (Figure 4.6B).
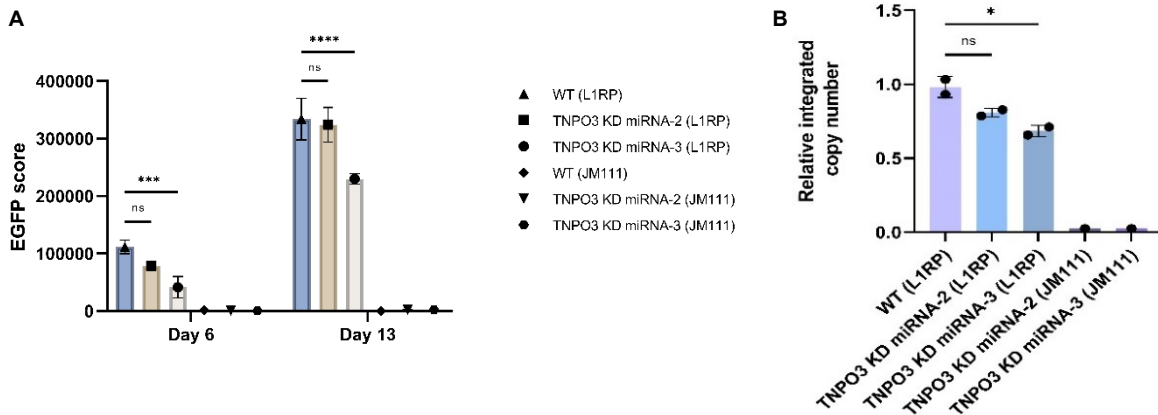

***Figure 4.6: LINE-1 retrotransposition assay with polyclonal TNPO3 KD miRNA-2 and TNPO3 KD miRNA-3 cells.
A. EGFP score for different cell lines on day 6 and 13 post-transfection.*** *WT HEK293T, polyclonal TNPO3 KD miRNA-2 and TNPO3 KD miRNA-3 cells were transfected with the L1RP plasmid or the JM111 plasmid using FuGENE6. Selection with puromycin was started at day 3 post-transfection. EGFP score (% EGFP positive cells x MFI) was determined on day 6 and 13 post-transfection. Transfection with the L1RP plasmid was performed in biological triplicate. Transfection with the JM111 plasmid was performed in biological duplicate. A significant decrease in LINE-1 retrotransposition was observed on day 6 and 13 post-transfection for polyclonal TNPO3 KD miRNA-3 cells. Two-way ANOVA followed by Dunnett's multiple comparison test was performed.* ***B. Relative integrated copy number of LINE-1 EGFP element.*** *On samples taken on day 13 post-transfection genomic DNA extraction was performed, followed by RT-qPCR. To determine the relative integrated copy number in the genome, primers flanking the γ-globin intron were used. B-actin was used as a reference gene. A significant decrease in integrated copy numbers was observed in polyclonal TNPO3 KD miRNA-3 cells. One-way ANOVA followed by Dunnett's multiple comparison test was used. Analysis was performed in biological duplicate. Error bars: SD. ns: not significant; *: p < 0.05; ***: p < 0.001; ****: p < 0.0001.*

This experiment was repeated with polyclonal TNPO1 KD and TNPO3 KD cells by following the same procedure. Samples for flow cytometry were taken on day 6, 10 and 13 post-transfection. Flow cytometry analysis showed a significant decrease in LINE-1 retrotransposition on day 13 post-transfection in both the polyclonal TNPO1 KD and TNPO3 KD cells. The decrease on day 6 and 10 post-transfection was not significant (Figure 4.7A).

Third, monoclonal TNPO1 KD (clone 15) and TNPO3 KD (clone 6) cells, with the strongest KD, were examined for their effect on LINE-1 activity. The same procedure was followed as for the previous LINE-1 retrotransposition assays. Samples were taken on day 6 and 13 post-transfection to perform flow cytometry. Data revealed a significant decrease in LINE-1 activity for both of the monoclonal cell

lines on day 13 post-transfection. A non-significant decrease was observed on day 6 post-transfection (Figure 4.7B). The relative integrated copy number in the genomic DNA was determined at day 13 post-transfection for the WT and monoclonal TNPO1 KD cells. A significant decrease in the relative integrated copy number was obtained for the monoclonal TNPO1 KD cells (Figure 4.7C).
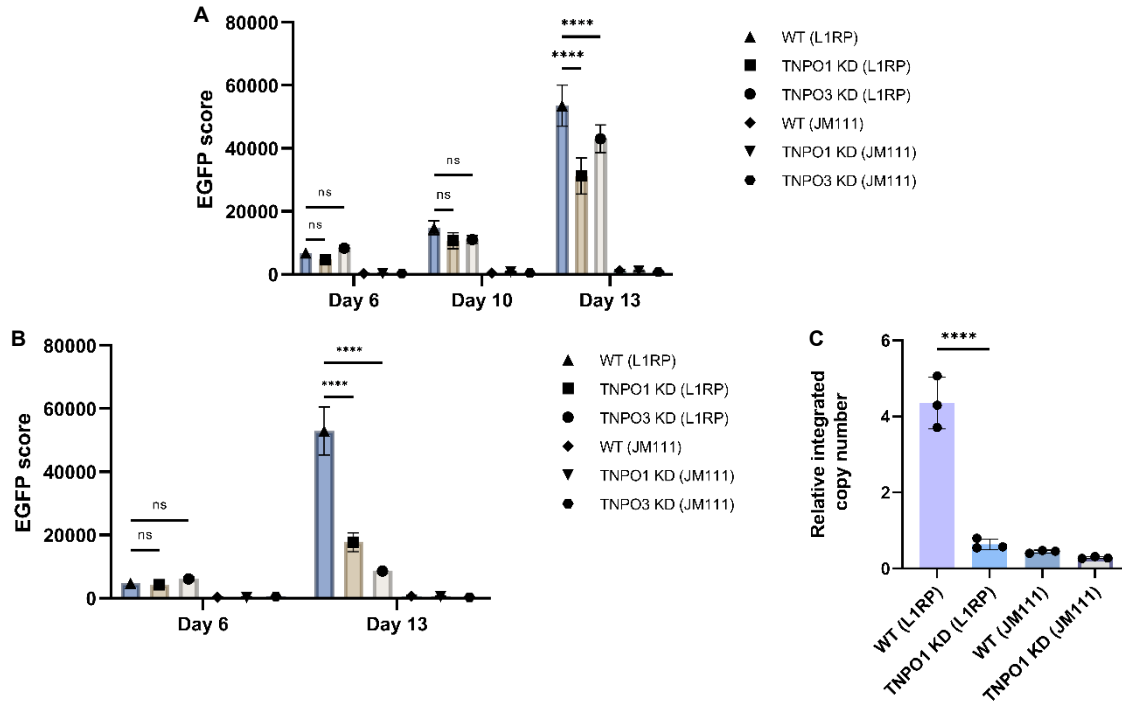

*Figure 4.7: LINE-1 retrotransposition assay with TNPO1 KD and TNPO3 KD cells. A. LINE-1 retrotransposition assay with polyclonal TNPO1 KD and TNPO3 KD cell lines. WT HEK293T, polyclonal TNPO1 KD and TNPO3 KD cells were transfected with the L1RP plasmid or the JM111 plasmid using FuGENE6. Selection with puromycin was started at day 3 post-transfection. EGFP score (% EGFP positive cells x MFI) was determined at day 6, 10 and 13 post-transfection. A significant decrease in LINE-1 retrotransposition was observed in polyclonal TNPO1 KD and TNPO3 KD cells at day 13 post-transfection. Experiments were performed in biological triplicate. Two-way ANOVA followed by Dunnett's multiple comparison test was performed. B. LINE-1 retrotransposition assay with monoclonal TNPO1 KD and TNPO3 KD cell lines. The same procedure was followed as described in A, with monoclonal TNPO1 KD and TNPO3 KD cells. EGFP score (% EGFP positive cells x MFI) was determined at day 6 and 13 post-transfection. A significant decrease in LINE-1 retrotransposition was observed in monoclonal TNPO1 KD and TNPO3 KD cells at day 13 post-transfection. Analysis was performed in biological triplicate. Two-way ANOVA followed by Dunnett's multiple comparison test was performed. C. Relative integrated copy number of LINE-1 element. Genomic DNA extraction was performed on samples taken on day 13 post-transfection followed by RT-qPCR. The relative integrated copy number in the genome was determined with primers flanking the γ-globin intron. A significant decrease in integrated copy numbers was observed in monoclonal TNPO1 KD cells. One-way ANOVA followed by Dunnett's multiple comparison test was used. Analysis was performed in biological triplicate. Error bars: SD. ns: not significant; ****: $p < 0.0001$.*

4.1.5 The endogenous ORF1p expression in HEK293T cell lines

The endogenous expression of the ORF1p was determined in both polyclonal and monoclonal TNPO1 KD and TNPO3 KD cells. Western Blot was performed with the whole-cell lysate to reveal the expression of the ORF1p in these cell lines. No decrease in the ORF1p expression was observed in either of the TNPO1 KD and TNPO3 KD cell lines (Figure 4.8).

Figure 4.8: Determination of the endogenous ORF1p expression in TNPO1 KD and TNPO3 KD cells on Western Blot. Whole-cell lysate of WT HEK293T cells, poly- and monoclonal TNPO1 KD and TNPO3 KD cells was loaded at a final amount of 20 µg of protein. Vinculin was used as a loading control and gives a band at a height of 133 kDa. The ORF1p was detected at a height of 44 kDa and is equally expressed in all tested cell lines.
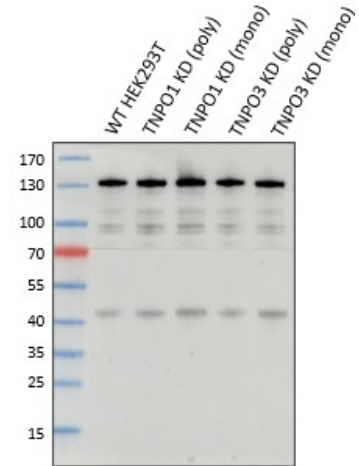
4.2 OPTIMIZATION OF LINE-1 ASSAY IN SH-SY5Y CELLS

4.2.1 Liposome-mediated transfection in SH-SY5Y cells

SH-SY5Y cells are difficult to transfect. However, different transfection reagents are available that can be tested for their transfection efficiency in this hard-to-transfect cell line. During this master thesis, different transfection reagents were tested to obtain a transfection efficiency in WT SH-SY5Y cells that is sufficient to perform the full LINE-1 assay.

A first try was given with FuGENE6 as a transfection reagent. FuGENE6 is also the transfection reagent that is used in the LINE-1 retrotransposition assay performed in HEK293T cells. SH-SY5Y cells were plated at a density of 3.5×10^4 cells/well in a 48-well plate. After 24 h, each well was co-transfected with a GFP mock reporter plasmid and the L1RP plasmid using FuGENE6 in different ratios of FuGENE6:DNA based on literature (87, 88) and the protocol of the manufacturer. On day 2 post-transfection, samples were taken for flow cytometry and the percentage of GFP positive cells was determined for each well. The highest transfection efficiency was obtained for the ratio of 4.5:1 FuGENE6:DNA, with an efficiency of 21.14 % (Figure 4.9A).

The full LINE-1 retrotransposition assay was performed with FuGENE6 as a transfection reagent. WT SH-SY5Y cells were plated in a 48-well plate at a density of 3.5×10^4 cells/well. Cells were transfected with either the L1RP plasmid or the JM111 plasmid as a negative control in a ratio of 4.5:1 FuGENE6:DNA. From day 2 post-transfection, transfected cells were selected with puromycin. On day

6, 9, 13, 16 and 20 post-transfection samples for flow cytometry were taken. A non-significant difference in the EGFP score was obtained between both conditions (Figure 4.9B). A possible explanation for this non-significant difference could be that no selection occurred of the transfected cells. Another explanation could be that the percentage of transfected cells is too low to outcompete the non-transfected cells since SH-SY5Y cells need cell-to-cell communication to grow well (89).

To achieve a higher transfection efficiency, other transfection reagents were tested. LipofectamineLTX and Lipofectamine3000 were available in the host lab and following the protocol of the manufacturer, different ratios of reagent:DNA were tested. Here, WT SH-SY5Y cells were seeded in a 48-well plate at a density of 5×10^4 cells/well. Cells were co-transfected with a GFP mock reporter plasmid and the L1RP plasmid using LipofectamineLTX or Lipofectamine3000. Samples for flow cytometry were taken on day 2 post-transfection and the transfection efficiency was determined based on the percentage of GFP positive cells per well. For LipofectamineLTX, the highest transfection efficiency, 5.1 %, was obtained for the ratio of 2:1 LipofectamineLTX:DNA (Figure 4.10A). The ratio of 1.5:1 Lipofectamine3000:DNA gave the best transfection efficiency of 28.2 % (Figure 4.10B).
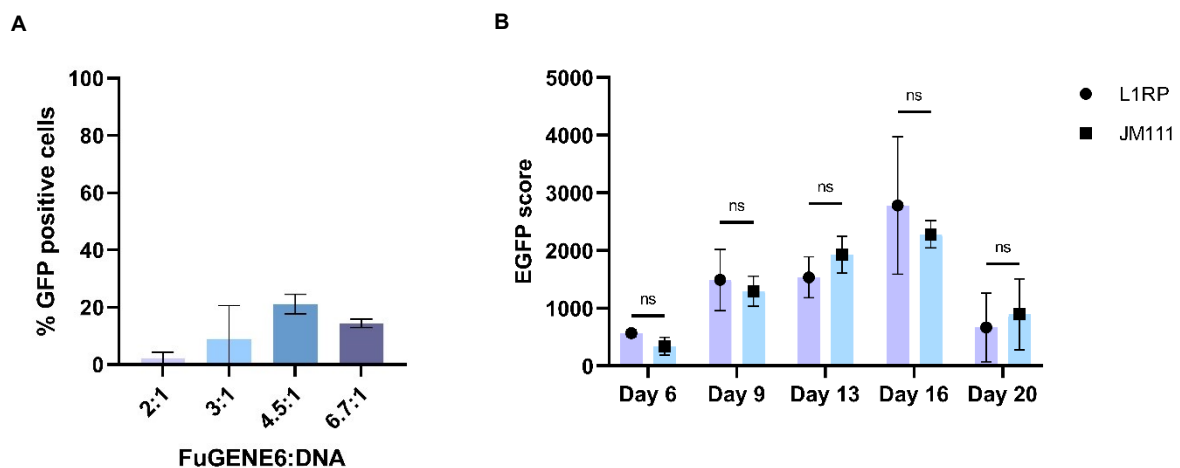

Figure 4.9: Transfection of WT SH-SY5Y cells with FuGENE6. A. FuGENE6 in different ratios. *Transfection efficiency was determined by co-transfecting a GFP mock reporter plasmid with the L1RP plasmid. At 2 days post-transfection, the percentage of GFP positive cells was determined by flow cytometry. A transfection efficiency of 21.14 % was obtained for the ratio of 4.5:1 FuGENE6:DNA. Transfections were performed in biological duplicate.* **B. LINE-1 retrotransposition assay in WT SH-SY5Y cells.** *WT SH-SY5Y cells were transfected with the L1RP or the JM111 plasmid using FuGENE6 in a ratio of 4.5:1 FuGENE6:DNA. From day 2 post-transfection, cells were selected with puromycin. The EGFP score (% EGFP positive cells x MFI) was estimated at day 6, 9, 13, 16 and 20 post-transfection. A non-significant difference between the L1RP and the JM111 plasmid was obtained. Transfections were performed in biological triplicate. Two-way ANOVA followed by Sidak's multiple comparison test was performed. Error bars: SD; ns not significant.*
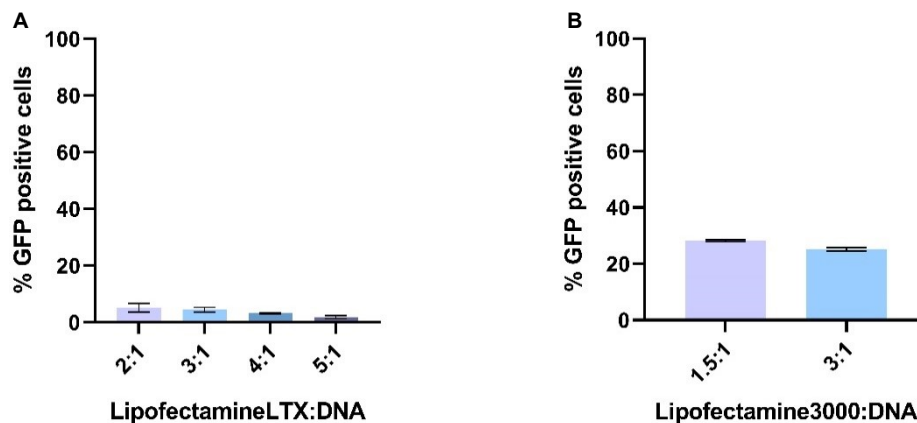
Figure 4.10: Transfection efficiency with LipofectamineLTX or Lipofectamine3000. A. LipofectamineLTX in ***different ratios.*** *Cells were co-transfected with the L1RP plasmid and a GFP mock reporter plasmid. At 2 days post-transfection, flow cytometry was used to determine the percentage of GFP positive cells. The highest transfection efficiency of 5.1 % was obtained for the ratio of 2:1 LipofectamineLTX:DNA. Transfections were performed in biological duplicate. **B. Lipofectamine3000 in different ratios.** The same procedure was followed, but by making use of Lipofectamine3000 in different ratios. In the ratio of 1.5:1 Lipofectamine3000:DNA, a transfection efficiency of 28.2 % was obtained. Transfections were performed in biological duplicate. Error bars: SD.*

It was decided to continue with Lipofectamine3000 as a transfection reagent and to try an upscaling of the procedure. Now, WT SH-SY5Y cells were plated in a 24-well plate at a density of 1×10^5 cells/well. After 24 h, cells were co-transfected with a GFP mock reporter plasmid and the L1RP plasmid or the JM111 plasmid using Lipofectamine3000 in a final ratio of 1.5:1 Lipofectamine3000:DNA. The number of GFP positive cells was determined on day 2 post-transfection and resulted in a transfection efficiency of 44.8 and 38.9 % for the L1RP and the JM111 plasmid respectively (Figure 4.11A).

By making use of Lipofectamine3000, a transfection efficiency of about 40 % was obtained, which should be sufficient to carry out the full LINE-1 retrotransposition assay. WT SH-SY5Y cells were transfected with the L1RP or the JM111 plasmid as a negative control. From day 3 post-transfection, transfected cells were selected with 1 µg/mL puromycin. No selection had occurred on day 8 post-transfection. It was decided to increase the concentration of puromycin to 3 µg/mL. However, on day 9 post-transfection all the transfected conditions were dead. No samples for readout could be taken. A repeat was performed of the experiment, but now 1.5 or 2 µg/mL of puromycin was used to select the transfected cells. Again, all the cells of the transfected conditions were dead after selection with puromycin.

Since the GFP mock reporter plasmid is only 6 kb in size and the L1RP or the JM111 plasmid is 18 kb in size, it is possible that the obtained transfection efficiency is solely representative for the smaller GFP mock reporter plasmid. Therefore, transfection efficiency was determined for the LRRK2-EGFP plasmid that is 18 kb in length and allows to determine the EGFP positive cells at day 2 post-transfection. SH-SY5Y cells were seeded at a density of 2×10^5 cells/well. Cells were co-transfected with a GFP mock reporter plasmid and the L1RP plasmid or transfected with the LRRK2-EGFP plasmid, 24 h after seeding. The percentage of GFP or EGFP positive cells was determined at day 2 post-transfection and resulted in a transfection efficiency of 29.31 and 6.4 % for the co-transfection with the GFP mock reporter plasmid and the transfection with the LRRK2-EGFP plasmid respectively (Figure 4.11B). It seems that liposome-mediated transfection does not work in SH-SY5Y cells and does not result in the desired transfection efficiency.
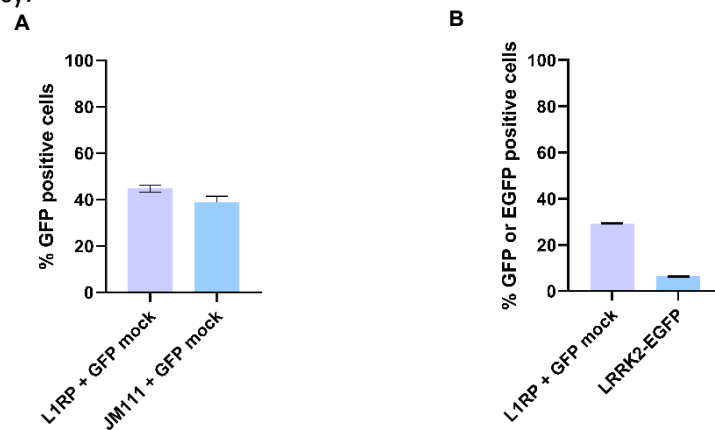

Figure 4.11: Optimization of transfection efficiency with Lipofectamine3000. A. Transfection efficiency for Lipofectamine3000. *The L1RP or the JM111 plasmid was co-transfected with a GFP mock reporter plasmid. The percentage of GFP positive cells was determined on day 2 post-transfection. A transfection efficiency of 44.8 % was determined for the L1RP plasmid and a transfection efficiency of 38.9 % was determined for the JM111 plasmid. Transfections were performed in biological duplicate.* ***B. Transfection efficiency of LRRK2-EGFP plasmid.*** *Cells were co-transfected with the L1RP plasmid and a GFP mock reporter plasmid or transfected with the LRRK2-EGFP plasmid. The percentage of GFP or EGFP positive cells was determined 2 days post-transfection. A transfection efficiency of 6.4 % was obtained for the LRRK2-EGFP plasmid. Transfections were performed in biological duplicate. Error bars: SD.*

4.2.2 Nucleofection of SH-SY5Y cells

Besides liposome-mediated transfection, nucleofection is another available method to perform transfection of SH-SY5Y cells. In this method, electroporation and cell-type-specific reagents are combined to achieve higher transfection efficiencies (90).

First, 2 x 10^6 WT SH-SY5Y cells were used to perform nucleofection. The protocol of the manufacturer was followed and different conditions were tested. The supplied pmaxGFP® vector was used in a final amount of 2 µg of DNA. Analogously, 2, 4 or 6 µg of the LRRK2-EGFP plasmid was tested. 2 days after nucleofection, samples were taken to determine GFP or EGFP positive cells by flow cytometry. A transfection efficiency of 65.7 % was achieved for the pmaxGFP® vector (Figure 4.12A). For the LRRK2-EGFP, the highest transfection efficiency, 2.4 %, was obtained with 4 µg of the LRRK2-EGFP plasmid (Figure 4.12A).

To further optimize the nucleofection protocol, different cell densities were tested for their effect on the transfection efficiency. Now, 1 x 10^6 or 1.5 x 10^6 WT SH-SY5Y cells were transfected with 2 µg of the supplied pmaxGFP® vector or 4 µg of the LRRK2-EGFP plasmid. Samples to determine GFP or EGFP positive cells were taken 48 h and 72 h after nucleofection. In the conditions of 1 x 10^6 WT SH-SY5Y cells, a transfection efficiency of 38.3 % or 1.5 % was achieved for the pmaxGFP® or the LRRK2-EGFP plasmid respectively at 72 h after nucleofection (Figure 4.12B). A transfection efficiency of 41.9 % or 1.8 %, for the pmaxGFP® vector or LRRK2-EGFP plasmid respectively, was obtained for the conditions with 1.5 x 10^6 WT SH-SY5Y cells at 72 h after nucleofection (Figure 4.12C).
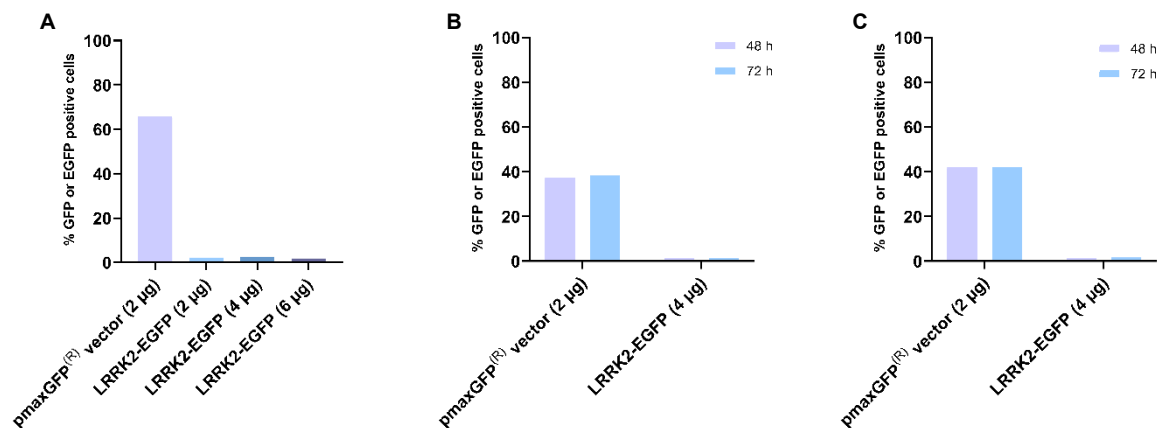

Figure 4.12: Nucleofection of SH-SY5Y cells. A. Nucleofection of 2 x 10^6 SH-SY5Y cells. SH-SY5Y cells were transfected with the pmaxGFP® vector or the LRRK2-EGFP plasmid by nucleofection. 2 days after nucleofection, the percentage of GFP or EGFP positive cells was determined by flow cytometry. A transfection efficiency of 65.7 % was achieved for the pmaxGFP® vector and an efficiency of 2.1, 2.4 or 1.8 % was obtained for 2 µg, 4 µg or 6 µg of the LRRK2-EGFP plasmid. B. Nucleofection of 1 x 10^6 SH-SY5Y cells. Nucleofection was performed with 2 µg of the pmaxGFP® vector or 4 µg of the LRRK2-EGFP plasmid. The percentage of GFP or EGFP positive cells was determined 48 h and 72 h after nucleofection. A transfection efficiency of 37.4 and 38.3 % was achieved for the pmaxGFP® vector, 48 and 72 h after nucleofection respectively. For the LRRK2-EGFP plasmid an efficiency of 1.3 and 1.5 % was obtained 48 h and 72 h after nucleofection. C. Nucleofection of 1.5 x 10^6 SH-SY5Y cells. The same procedure was followed as in B. For the pmaxGFP® vector, a transfection efficiency of 41.9 % was achieved 48 and 72 h after nucleofection. A transfection efficiency of 1.5 and 1.8 % was obtained for the LRRK2-EGFP plasmid 48 and 72 h after nucleofection.

4.3 OPTIMIZATION OF THE ORF1P STAINING ON MOUSE BRAIN SLICES

The detection of endogenous levels of the ORF1p is of importance when expression levels need to be defined in different PD mouse models. Immunohistochemical and immunofluorescent stainings were performed on coronal brain slices of C57BL/6J WT mice of different ages. Stainings were carried out with the help of a lab technician in the host lab.

4.3.1 Immunohistochemical staining

In a first attempt, immunohistochemistry was performed with the monoclonal anti-LINE-1 ORF1p antibody in a dilution of 1/500. This staining revealed an expression of the ORF1p in the cytoplasm of the cells that are present in the hippocampus, cortex and substantia nigra (Figure 4.13A-C). Staining of the testis was performed as a positive control since it is known that a high expression of the ORF1p is present in spermatocytes (67) (Figure 4.13D). In this staining, the signal was quite weak and a lot of background staining was present too.
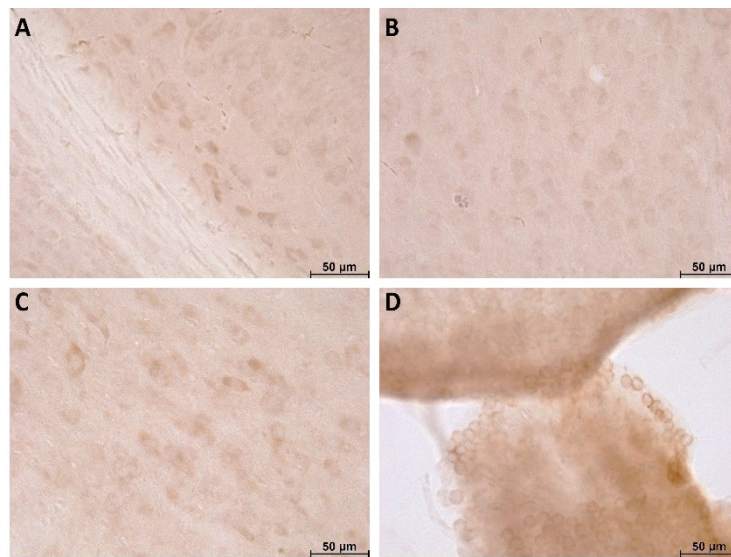
Figure 4.13: Endogenous expression of the ORF1p in 4-week old WT mouse. A-C. Immunohistochemical staining for the ORF1p on coronal brain slice of a WT mouse. Before staining, antigen retrieval was performed with citrate buffer. Afterwards, the brain slice was treated with the primary anti-LINE-1 ORF1p antibody (1/500). As a secondary antibody, biotinylated anti-rabbit IgG was used, followed by incubation with streptavidin-horseradish peroxidase complex. DAB was used as a chromogen to visualize the ORF1p. The ORF1p was detected in the cytoplasm of cells present in the hippocampus (A), cortex (B) and substantia nigra (C). D. Immunohistochemical staining for the ORF1p in the testis of a WT mouse. Since it is known that the spermatocytes express the protein of interest, staining on the testis was used as a positive control. Magnification = 40x. Scale bar = 50 μm.

In a second attempt, the antibody was used in a dilution of 1/100. Extra wash steps were performed to lower the background signal. Again, the expression of the ORF1p was observed in the cytoplasm of the cells present in the substantia nigra (Figure 4.14). The background signal was reduced, but still present.
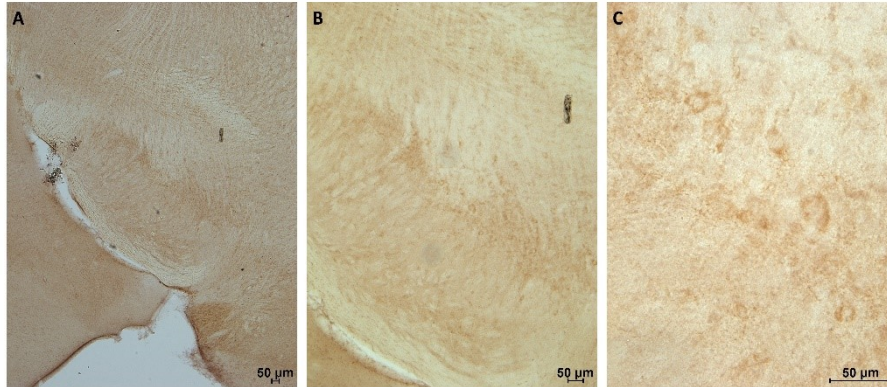

Figure 4.14: Endogenous expression of the ORF1p on coronal brain slice of 8-week old WT mouse. A-C. Immunohistochemical staining for the ORF1p in the substantia nigra of a WT mouse. Antigen retrieval was performed with citrate buffer. Primary anti-LINE-1 ORF1p antibody was used in a dilution of 1/100. Biotinylated anti-rabbit IgG was used as a secondary antibody and slices were incubated with streptavidin-horseradish peroxidase complex. DAB was used as a chromogen to visualize the ORF1p. The ORF1p was detected in the cytoplasm of cells present in the substantia nigra. Magnification = 5X (A), 10X (B) or 40X (C). Scale bar = 50 µm.

4.3.2 Immunofluorescent staining

A dilution of 1/500 of the anti-LINE-1 ORF1p antibody was used for the immunofluorescent staining of the coronal brain slice of a 4-week old WT mouse. The nuclear staining with DAPI was also included. This staining revealed expression of the ORF1p in the cytoplasm of cells which are present in the hippocampus, cortex and substantia nigra (Figure 4.15A-C). Similar to the DAB staining, immunofluorescent staining of the testis was included as a positive control for the ORF1p expression (67) (Figure 4.15D). Staining was visualized on a fluorescence microscope.

The substantia nigra is characterized by the presence of numerous dopaminergic neurons. To verify if the ORF1p is expressed in these neurons, double staining with an antibody against tyrosine hydroxylase was performed. Besides, the shape of the cells that were ORF1p positive in the previous staining, is reminiscent for neurons (Figure 4.14 – 4.15C). The anti-LINE-1 ORF1p antibody was used in a dilution of 1/100. Stainings were checked on a fluorescence and confocal microscope. The merged image taken with the fluorescence microscope showed an expression of the ORF1p in the dopaminergic neurons that are present in the substantia nigra (Figure 4.16A). Due to the prominent background, it was hard to detect the expression of the ORF1p. The same staining was also visualised

with confocal microscopy. This revealed that the ORF1p is expressed in all the dopaminergic neurons that are located in the substantia nigra. The merged image shows a clear overlap for the dopaminergic neurons together with the ORF1p expression (Figure 4.16B). It is important to note that not all the ORF1p positive cells are dopaminergic neurons, but some other cells in the substantia nigra are also ORF1p positive (Figure 4.16B).
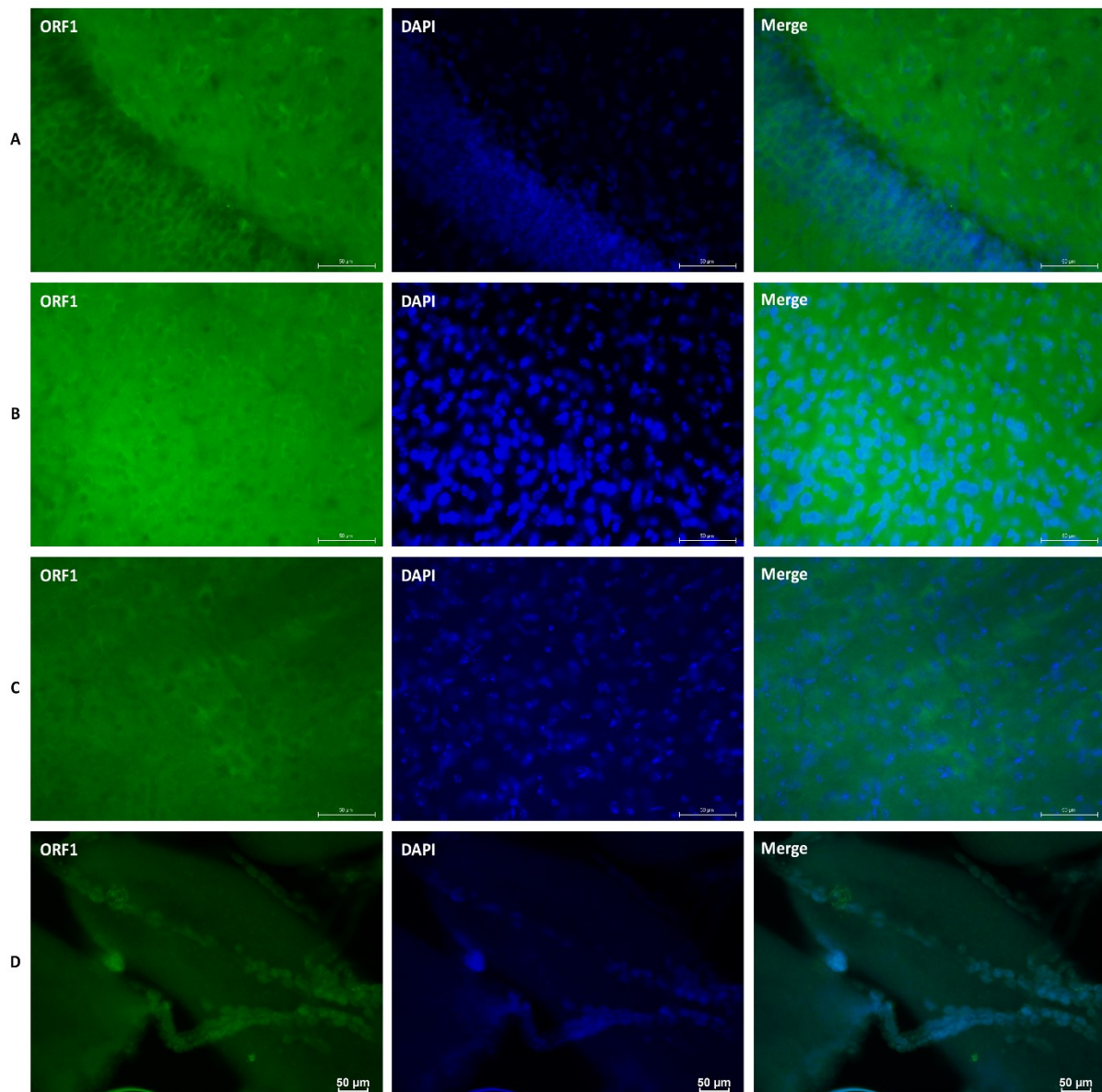
Figure 4.15: Endogenous expression of the ORF1p in 4-week old WT mouse. A-C. Immunofluorescent staining for the ORF1p on coronal brain slice of a WT mouse. Antigen retrieval with citrate buffer was performed prior to staining. Anti-LINE-1 ORF1p (1/500) antibody was used as a primary antibody to treat the brain slice. Fluorochrome-conjugated anti-rabbit Alexa 488 IgG was used as a secondary antibody. Slices were covered with Mowiol and DAPI. Images were taken on a fluorescence microscope. ORF1p was detected in the cytoplasm of the cells present in the hippocampus (*A*), cortex (*B*) and substantia nigra (*C*). Magnification= 40x. Scale bar = 50 µm. *D. Immunofluorescent staining for the ORF1p in the testis of a WT mouse.* Staining for the ORF1p in the testis was used as a positive control. Magnification= 20x. Scale bar = 50 µm.
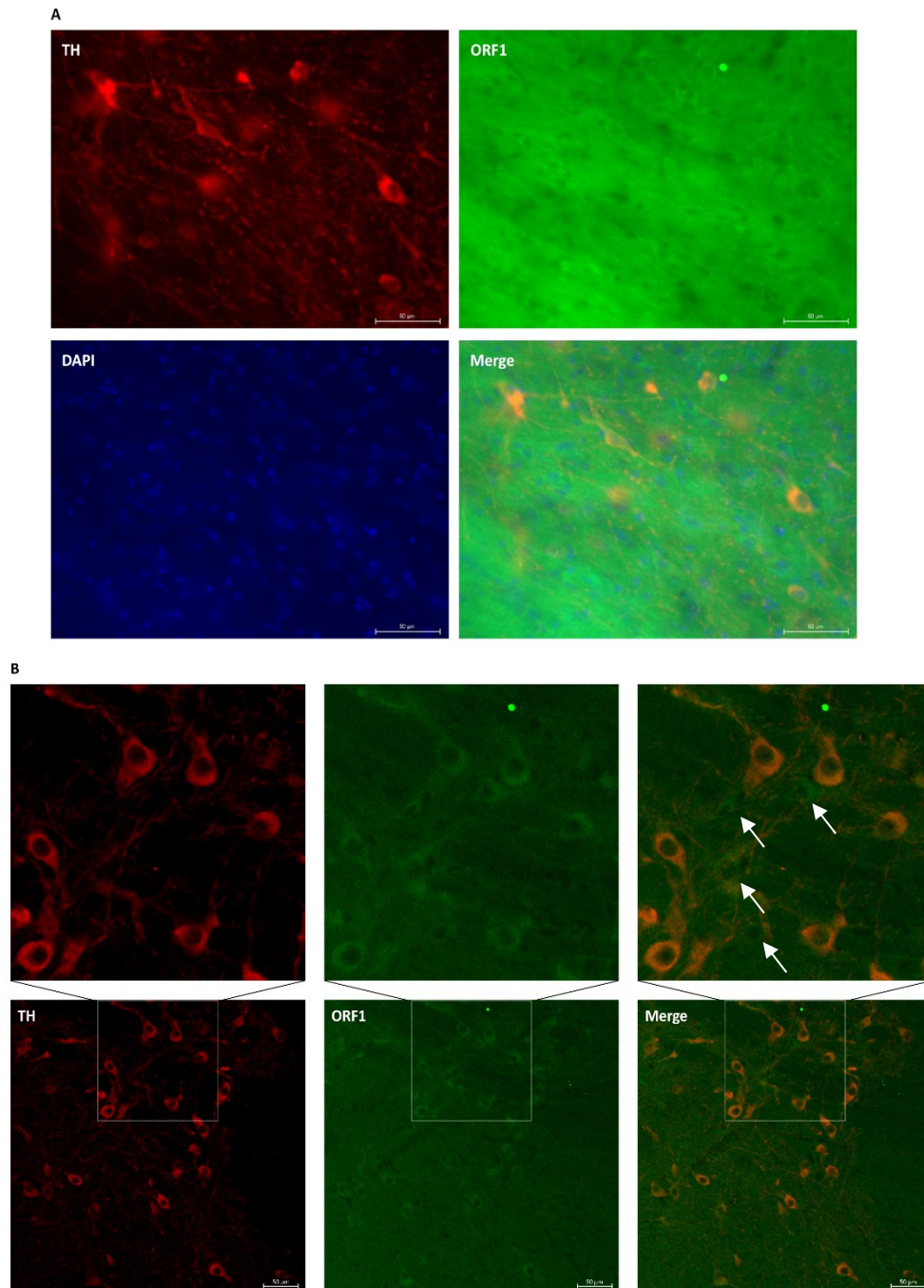
Figure 4.16: Double staining for TH and the ORF1p in substantia nigra of 8-week old WT mouse.
A. Immunofluorescent staining on coronal brain slice of a WT mouse. *Antigen retrieval was performed with the citrate buffer prior to incubation with primary anti-TH (1/1000) and anti-LINE-1 ORF1p (1/100) antibody. Fluorochrome-conjugated anti-rabbit Alexa 555 or Alexa 488 IgG were used as secondary antibodies. Slices were mounted with a coverslip with Mowiol and DAPI. Images taken with fluorescence microscope revealed expression of the ORF1p in TH positive cells present in the substantia nigra. Magnification= 40x. Scale bar = 50 μm.* ***B.***
Immunofluorescent staining on coronal brain slice of a WT mouse. *The coronal brain slice was also visualized with confocal microscopy. Results revealed the expression of the ORF1p in the TH positive cells in the substantia nigra. White arrows indicate non-dopaminergic cells present in the substantia nigra that are positive for expression of the ORF1p. Magnification= 20x. Scale bar = 50 μm.*

5 DISCUSSION

5.1 TNPO1 AND TNPO3 AS HOST FACTORS OF LINE-1

The results in this master thesis support the hypothesis that TNPO1 and TNPO3 are potential host factors involved in the nuclear import of the LINE-1 RNP complex. A decrease in LINE-1 retrotransposition was observed when performing the LINE-1 retrotransposition assay with TNPO1 KD and TNPO3 KD cell lines (Figure 4.6 – 4.7). The results obtained for TNPO1 KD cells confirm the findings of the research group of Dr. I. Pedersen (48). Besides, the data obtained for TNPO3 KD cell lines in the LINE-1 retrotransposition assay are the first to demonstrate a potential role of TNPO3 in LINE-1 retrotransposition. The EGFP score and/or the relative integrated copy number were utilised as a readout for LINE-1 retrotransposition. The decrease in LINE-1 retrotransposition on day 13 post-transfection was more pronounced in the assay performed with the monoclonal TNPO1 KD and TNPO3 KD cell lines compared to the polyclonal TNPO1 KD and TNPO3 KD cell lines (Figure 4.7B). A possible explanation for this observed difference is the higher level of depletion on the mRNA and protein level for the monoclonal cell lines compared to the polyclonal cell lines (Figure 4.3 – 4.4). In line with the data obtained by flow cytometry, the relative integrated copy number also revealed a decrease in LINE-1 retrotransposition for the TNPO1 KD and TNPO3 KD cell lines.

Initially, there was no decrease in LINE-1 retrotransposition observed for the polyclonal TNPO3 KD miRNA-2 cell line compared to the WT HEK293T cells on day 13 post-transfection, whereas the polyclonal TNPO3 KD miRNA-3 cell line resulted in a significant decrease (Figure 4.6). Interestingly, the polyclonal TNPO3 KD miRNA-2 cell line showed a higher level of KD on the mRNA and protein level of TNPO3 compared to the polyclonal TNPO3 KD miRNA-3 cell line. However, when further performing the LINE-1 retrotransposition assay with the polyclonal TNPO3 KD miRNA-2 cell line, a significant decrease in LINE-1 retrotransposition was obtained on day 13 post-transfection (Figure 4.7A). A possible explanation for the observed difference could be contamination of the TNPO3 KD miRNA-2 cell line with WT HEK293T cells.

Since it is proven that LINE-1 retrotransposition takes place in nondividing neurons (23), there should be other mechanisms by which the LINE-1 RNP complex access the DNA independently of cell division. Of note, both TNPO1 and TNPO3 are renowned as nuclear import factors. Taking into account the obtained results in the LINE-1 retrotransposition assay with the TNPO1 KD and TNPO3 KD cell lines, it can be suggested that both proteins play a role in the nuclear import of the LINE-1 RNP complex.

In other words, TNPO1 and TNPO3 are helping the LINE-1 RNP complex to gain access to the DNA in the nucleus.

To exclude that the KD of TNPO1 or TNPO3 is toxic for HEK293T cells, growth curves were obtained. No significant difference in cell proliferation was found for the different HEK293T cell lines (Figure 4.5). Therefore, it can be excluded that the observed decrease in LINE-1 retrotransposition is caused by lower viability of the TNPO1 KD and TNPO3 KD cell lines.

Next, the endogenous expression of the ORF1p was determined on the whole-cell lysate of various HEK293T cells. We hoped to observe a decrease in the ORF1p expression in the TNPO1 KD and TNPO3 KD cell lines. If TNPO1 and TNPO3 are involved in the nuclear import of the LINE-1 RNP complex, then fewer rounds of endogenous *de novo* LINE-1 retrotransposition will occur in the TNPO1 KD and TNPO3 KD cell lines. It would mean that less LINE-1 mRNA will be produced, resulting in less expression of the ORF1p. However, no difference was observed in the ORF1p expression on Western Blot (Figure 4.8). An explanation of the observed result could be that there is no high rate of *de novo* LINE-1 retrotransposition in HEK293T cells, meaning that the decrease in LINE-1 retrotransposition in the TNPO1 KD and TNPO3 KD cell lines compared to WT HEK293T cells is too low to be detected on Western Blot. In addition, due to a lower nuclear import of the LINE-1 RNP complex, an accumulation of the ORF1p can occur in the cytoplasm. Since the whole-cell lysate was used for this Western Blot, it is possible that the difference was not detected. In the future, it would be interesting to perform a Western Blot on the nuclear and cytoplasmic fraction of the various cell lines.

The role of TNPO1 in LINE-1 retrotransposition was investigated before by the research group of Dr. I. Pedersen. They showed that miRNA-128 has a direct and indirect effect on LINE-1 retrotransposition. The direct effect on LINE-1 retrotransposition is due to the binding of miRNA-128 to the LINE-1 ORF2 RNA resulting in an inhibition of the translation of the ORF2p (91). Recently, they revealed that miRNA-128 is also able to indirectly inhibit LINE-1 retrotransposition by downregulation of TNPO1 (48). First, they confirmed the decrease in LINE-1 retrotransposition in HeLa cells stably transduced with a lentiviral vector expressing miRNA-128. Binding targets of miRNA-128 were searched in view to determine an indirect effect of miRNA-128 by downregulation of host factors involved in LINE-1 retrotransposition. TNPO1 was identified as a binding target of miRNA-128 and a decrease in TNPO1 expression was obtained in the transduced HeLa cells (48). Next, TNPO1 KD HeLa cells were created by transduction with a lentiviral vector encoding a TNPO1-specific shRNA. To investigate whether the depletion of TNPO1 is also partially responsible for the decrease in LINE-1 retrotransposition, the colony formation assay was performed. Indeed, a decrease was observed in LINE-1 retrotransposition for the TNPO1 KD HeLa cells (48). A HeLa cell line overexpressing the TNPO1 gene was also created and

tested in the colony formation assay. An increase in colonies was observed, which means that more LINE-1 retrotransposition had occurred (48). The interaction between the TNPO1 and the ORF1-HA protein was revealed in a co-immunoprecipitation experiment but the exact characteristics of the interaction have yet to be identified (48).

The research group of Dr. I. Pedersen mentioned that miRNA-128 is also able to bind to the mRNA of TNPO3, resulting in downregulation of the TNPO3 gene (48). TNPO3 is renowned as a nuclear import factor of the pre-integration complex of HIV-1 (53). Taken the above into account, we investigated the potential role of TNPO3 in the nuclear import of the LINE-1 RNP complex.

5.1.1 Limitations and strengths

Here, the LINE-1 retrotransposition assay was performed with the LINE-1 EGFP reporter cassette which allowed us to utilise the EGFP score or relative integrated copy number of the LINE-1 EGFP element as a readout. The results in this master thesis confirm the findings obtained by the research group of Dr. I. Pedersen for TNPO1. The LINE-1 EGFP reporter cassette has the advantage of allowing rapid and easy detection of LINE-1 retrotransposition in a high-throughput and automated manner. Readout of LINE-1 retrotransposition can be obtained by flow cytometry and RT-qPCR on the genomic DNA. In contrast, the colony formation assay is more labour-intensive and less accurate. In this assay, it is important to remove the dead cells with PBS before counting the neomycin-resistant colonies. However, it is possible that some neomycin-resistant colonies are also removed by this PBS treatment, making the results of the counting less reliable. Another disadvantage of the colony formation assay is the need to manually count each colony under the microscope.

In this master thesis, the EGFP score was used as a readout for the data obtained by flow cytometry. The EGFP score is obtained by the percentage of EGFP positive cells multiplied with the MFI. Since the percentage of EGFP positive cells is only able to count the cells where one or multiple rounds of retrotransposition have occurred, the MFI was also taken into account resulting in the EGFP score. The advantage of including the MFI is that it gives an idea of the average fluorescence intensities from all the cells present in the sample. In addition, the relative integrated copy number of the LINE-1 EGFP element in the genomic DNA was also determined in some experiments (Figure 4.6B – 4.7C). RT-qPCR as a readout for LINE-1 retrotransposition has some advantages over the flow cytometry readout. First, the readout is not dependent on the expression of the EGFP gene. RT-qPCR allows detecting retrotransposition in restricted transcription regions of the genome in contrast to flow cytometry which needs the expression of the EGFP gene. Secondly, in RT-qPCR each retrotransposition event is detected whereas flow cytometry only gives an idea of how many cells contain at least one LINE-1

EGFP element. Thus, a more sensitive readout of LINE-1 retrotransposition can be achieved by RT-qPCR on the genomic DNA.

However, some limitations need to be taken into account when interpreting the obtained results. First, only the TNPO1 KD and TNPO3 KD cell lines were tested in the LINE-1 retrotransposition assay. Since these KD cell lines were created by transduction with a miRNA-based shRNA, it cannot be excluded that the off-targets of the miRNA are responsible for the observed decrease in LINE-1 retrotransposition. To ensure that the observed decrease is due to the KD of both genes and not the off-target effects of the miRNA, rescue cell lines need to be created. The rescue cell line can be created by transducing the TNPO1 KD or TNPO3 KD cell line with a viral vector encoding the full-length TNPO1 or TNPO3 gene, which is not targeted by the miRNA. The rescue cell lines should give an increase in LINE-1 retrotransposition compared to the KD cell lines in the assay. Upon rescue, the obtained results in KD cell lines will be validated. Second, it cannot be excluded that the observed decrease in LINE-1 retrotransposition with the TNPO3 KD cell line is due to an indirect effect of TNPO3. TNPO3 is responsible for the nuclear import of SR proteins, which are important during pre-mRNA splicing. An important step in the LINE-1 retrotransposition assay relies on the splicing of the LINE-1 mRNA at the intron that interrupts the EGFP reporter cassette. It is only possible to detect EGFP expression if this intron is removed. If fewer splicing factors are present in the nucleus due to the KD of TNPO3, it is possible that the mRNA is less spliced resulting in less detection of LINE-1 retrotransposition by EGFP expression. Eventually, there will still be retrotransposition, but this cannot be determined by EGFP expression.

5.1.2 Further perspectives

The data obtained in this master thesis support the hypothesis that TNPO1 and TNPO3 are involved in the nuclear import of the LINE-1 RNP complex during LINE-1 retrotransposition. However, the role of both proteins was only investigated by creating a KD cell line followed by performing the LINE-1 retrotransposition assay. The interaction between the ORF1-HA and TNPO1 protein is already corroborated by the research group of Dr. I. Pedersen, supporting the role of TNPO1 in the nuclear import of the LINE-1 RNP complex (48). For TNPO3, the interaction with LINE-1 is not yet identified. To exclude that the observed effect is caused by the limited nuclear import of SR proteins, the interaction between TNPO3 and LINE-1 has to be determined in future research. Co-immunoprecipitation between the LINE-1 proteins, the ORF1p or the ORF2p, and TNPO3 could give an idea of the interaction between both proteins. If an interaction is found then it can be excluded that the effect is only due to the decreased import of the splicing factors. In addition, it is known that TNPO3 plays an important

role in the nuclear import of the pre-integration complex of HIV-1 and interacts with the HIV-1 integrase (53). One of the activities of the HIV-1 integrase is endonucleolytic cleavage. Since the LINE-1 ORF2 encodes the ORF2p with EN activities, it can be hypothesised that TNPO3 interacts with the EN domain of the ORF2p. Further research on the interaction between TNPO3 and LINE-1 will help to determine the specific role of TNPO3 in LINE-1 retrotransposition.

The results of this master thesis provide preliminary results to identify TNPO1 and TNPO3 as host factors of LINE-1 retrotransposition. However, further research into the mechanism of action is needed to corroborate TNPO3 as nuclear import factor of the LINE-1 RNP complex.

5.2   TRANSFECTION OF SH-SY5Y CELLS

In order to study the biology of LINE-1 retrotransposition in the healthy and diseased human brain, the LINE-1 retrotransposition assay needs to be optimized in neuronal cells. In this thesis, the optimization of the assay in SH-SY5Y cells, a human neuroblastoma cell line, was tried. Optimization of the transfection efficiency is a crucial step before continuing with the full LINE-1 retrotransposition assay. It is also important to determine the transfection efficiency since the retrotransposition rates need to be corrected for the variation in these efficiencies. In this work, two different approaches of transfection were investigated, namely liposome-mediated transfection and nucleofection.

In the first part, liposome-mediated transfection was performed. This method relies on the formation of liposomes to efficiently transfer DNA into cells. Co-transfection with the L1RP plasmid and a GFP mock reporter plasmid was first tested with FuGENE6, the transfection reagent used in the LINE-1 retrotransposition assay in HEK293T cells. A transfection efficiency of 21.14 % was obtained and it was reasoned that this was high enough, since the transfected cells are selected afterwards (Figure 4.9A). However, a non-significant difference in EGFP score was observed between the L1RP and the JM111 plasmid when performing the full assay (Figure 4.9B). For this result, two explanations can be given. First, the transfected cells were too scarce to outcompete non-transfected cells. When SH-SY5Y cells don't have cell-to-cell communication, they don't grow very well. Second, cells were not transfected at all with the L1RP or the JM111 plasmid, resulting in the measurement of a background signal. Other transfection reagents were tested and Lipofectamine3000 resulted in a higher transfection efficiency than FuGENE6. A further upscaling of the procedure led to an efficiency of 44.8% for the co-transfection of the L1RP plasmid with the GFP mock reporter plasmid (Figure 4.11A). Again, the full LINE-1 retrotransposition assay was performed but resulted in no selection of the transfected cells after the addition of 1 µg/mL of puromycin. Also, the non-transfected cells survived the selection with

this concentration of puromycin. A higher concentration of puromycin resulted in the death of the transfected and non-transfected conditions. Indeed, the same explanations can be given for the LINE-1 retrotransposition assay performed with FuGENE6. However, it has to be kept in mind that the measured GFP positive cells are originating from the GFP mock reporter plasmid and not from the L1RP plasmid since there is some delay in the EGFP expression as a result of LINE-1 retrotransposition. The GFP mock reporter plasmid is only 6 kb in size, which is easier to transfect in comparison with the L1RP plasmid of 18 kb. In view to determine if the optimized transfection efficiency was only representative for the smaller GFP mock reporter plasmid, a larger EGFP plasmid, namely the 18 kb LRRK2-EGFP plasmid, was used to determine transfection efficiency. Here, only 6 % of the cells were transfected which explains why the full LINE-1 assay does not work in SH-SY5Y cells with liposome-mediated transfection (Figure 4.11B). Therefore, it was decided to stop liposome-mediated transfections and to try nucleofection in this master thesis. However, further optimization of the liposome-mediated transfection can potentially be achieved by varying cell density, testing other transfection reagents or varying the plasmid amounts.

Nucleofection is another method of transfection, where a combination of electric pulses and cell-type-specific reagents is used to introduce DNA into the cytoplasm and nucleus of cells. The manufacturer, Lonza, recommends optimizing the nucleofection protocol with their pmaxGFP® vector plasmid, which is only 4 kb in size. Since the L1RP plasmid is much larger in size, the LRRK2-EGFP plasmid was taken along to determine the transfection efficiency. For the pmaxGFP® vector plasmid, a high transfection efficiency was obtained but this was not the case for the LRRK2-EGFP plasmid (Figure 4.12A). Different cell densities were tested but did not result in higher transfection efficiency (Figure 4.12B-C). The use of a lower cell density per condition can induce the nucleofection reaction, but can also result in a lower survival rate. Nucleofection is based on electroporation, resulting in the creation of a temporary pore in the cell and nuclear membrane of cells. Therefore, it is not surprising that an 18 kb plasmid has more difficulties entering the cell through a pore, than a smaller 4 kb plasmid. Several approaches were tested, but we did not succeed in obtaining a high transfection efficiency for SH-SY5Y cells.

In literature, transfection efficiency is always determined by co-transfection of the L1RP or the JM111 plasmid with a GFP expression plasmid. For example, a hrGFP expression plasmid was used in the LINE-1 retrotransposition assay performed in HeLa cells (27). Another example is the use of the pEGFP-C1 expression plasmid to determine transfection efficiency (32). In the past, it was reported that SK-N-BE(2)-C cells, another human neuroblastoma cell line, are able to undergo retrotransposition. Here, LipofectamineLTX was used to perform the transfection with the L1RP and

the JM111 plasmid. Transfection efficiency was determined by co-transfection of the L1RP and the JM111 plasmid with the pEGFP-C1 expression plasmid, resulting in an efficiency of 40 % in this cell line (32). Based on our experience, we believe that this transfection efficiency resulted from the smaller EGFP reporter plasmid.

5.2.1 Limitations and strengths

During the first optimization steps, co-transfection of the L1RP plasmid with a GFP mock reporter plasmid was performed to determine transfection efficiency. Based on literature, it was initially believed to be the correct way to determine transfection efficiency. However, in the following experiments, the transfection efficiency was also determined in another way. The results in this master thesis are the first that investigate the real transfection efficiency in the LINE-1 retrotransposition assay. The 18 kb LRRK2-EGFP plasmid, where the EGFP gene is fused to the LRRK2 gene, is a representative plasmid to determine efficiency. In view of obtaining the expression of the EGFP gene, the full LRRK2 gene needs to be translated. A LINE-1 element is also large in size, which makes it a good reference to see what the real efficiency is. In HEK293T cells, the problem was never observed before, since they are easier to transfect and the retrotransposition assay did work in this cell line.

5.2.2 Further perspectives

In the future, further optimization of the transfection in the SH-SY5Y cells can be tried. On the one hand, the liposome-mediated transfection can be optimized by varying some parameters in the protocol, such as the cell density and transfection reagent. On the other hand, it is also possible to further optimize the nucleofection protocol in SH-SY5Y cells. Here, also a lot of parameters can be varied such as the cell density, the programme on the Nucleofector device and the amount of DNA. In addition, transfection would be easier to perform with a smaller LINE-1 plasmid, but the pCEP4 backbone cannot be minimized. All the elements present in the backbone are necessary to be able to carry out the LINE-1 retrotransposition assay. For example, EBNA-1 and OriP are necessary for the replication of the plasmid in cultured cells, resulting in a stable transfection of the plasmid. Another possibility is to deliver the LINE-1 EGFP reporter cassette via transduction with an adeno-associated vector. In the past, this was created once to study LINE-1 retrotransposition in nondividing somatic cells (92). It resulted in high levels of LINE-1 retrotransposition, but has not been used in further experiments to study LINE-1 retrotransposition. In the future, it can be interesting to further collaborate on the creation of a possible vector-based delivery method of the LINE-1 EGFP reporter cassette in hard-to-transfect cell lines, such as the SH-SY5Y cells.

5.3 THE ORF1P IS EXPRESSED IN THE BRAIN

In this master thesis, the endogenous expression of the ORF1p in the brain of WT mice is demonstrated. Expression of the ORF1p was detected in the cytoplasm of cells present in the hippocampus, cortex and substantia nigra of a 4-week old WT mouse both via immunohistochemical and immunofluorescent staining (Figure 4.13-4.15). Further optimization of the immunohistochemical staining on a coronal brain slice of an 8-week old WT mouse led to a reduction of the background signal. In addition, a more clear signal of the endogenous ORF1p expression was corroborated (Figure 4.14). Representative images of the double immunofluorescent staining with TH on a brain slice of an 8-week old WT mouse, revealed that the ORF1p is expressed in all dopaminergic neurons present in the substantia nigra. Besides, other cell types in the substantia nigra are ORF1p positive (Figure 4.16). However, no statistical analysis was performed on the images and only one brain slice was quantified. The obtained results with the double staining suggest that the ORF1p is expressed in all the dopaminergic neurons present in the substantia nigra. This is a potential result of a downregulation of MeCP2 in the dopaminergic neurons since MeCP2 acts as a repressor of LINE-1 retrotransposition (38). A double staining for TH and MeCP2 will give more clarity on the expression levels of MeCP2 in the dopaminergic neurons present in the substantia nigra.

The research group of Dr. A. Prochiantz has shown an increase of the ORF1p expression in the dopaminergic neurons of the *En1*-het mice, mice which are heterozygous for the allele of Engrailed-1 (67). In accordance with their data, expression of the ORF1p was seen in the hippocampus, cortex and substantia nigra of WT mice. Double staining with TH and ORF1p, revealed expression of the ORF1p to be higher in TH positive than in TH negative cells (67). However, their confocal images provoke some doubt on the signal detected for the ORF1p. The intensity of the ORF1p signal shows a lot of overlap with the signal obtained for TH, possibly through bleed-through of the TH signal. Bleed-through occurs when the fluorescent signal of a nearby channel is observed in the currently used channel on the confocal microscope.

5.3.1 Limitations and strengths

In our optimized ORF1p stainings, both the immunohistochemical and immunofluorescent staining of the coronal brain slices, the background is still prominently present. However, a weak signal of the ORF1p could be detected despite the background. Antigen retrieval was performed prior to staining to unmask the antigen and to make detection of the endogenous ORF1p possible. It has to be kept in mind that here the endogenous levels of the ORF1p expression were detected explaining in some part

the quite weak signal for the ORF1p. In addition, the specificity of the antibody against the LINE-1 ORF1p was confirmed by staining of the spermatocytes since they have a high expression of the ORF1p (67).

In the double staining, secondary antibodies conjugated with the Alexa Fluor 488 and Alexa Fluor 555 were used which show a small spectral overlap. The signal detected for the ORF1p in TH positive neurons could be originating from the bleed-through of the strong TH signal. However, images taken on the confocal microscope showed ORF1p positive cells in the substantia nigra which are not TH positive (Figure 4.16B). Approximately the same fluorescence intensities of the ORF1p signal were detected for TH positive and negative cells. As shown by the research group of Dr. A. Prochiantz, the ORF1p expression in dopaminergic neurons was visualised. However, the confocal images in this master thesis can exclude the bleed-through of the TH signal, which is not the case for the research group of Dr. A. Prochiantz. A limitation of the double staining is that no quantitative analysis can be performed to determine if all the dopaminergic neurons in the substantia nigra express the ORF1p. Stainings were performed on a single coronal brain slice from a single mouse which do not allow statistical analysis. In the future, more coronal brain slices originating from more than one mouse should be included to be able to perform a statistical analysis.

5.3.2 Further perspectives

Since there is still a background signal present in the immunofluorescent staining of the coronal brain slices, further optimization can be achieved by using a quenching solution. It is known that some cell compartments, such as the extracellular matrix and lipofuscin, are responsible for autofluorescence, giving rise to a background signal in immunofluorescent stainings (93). Adding a quenching solution to the staining, will probably result in a weaker background signal due to lower autofluorescence. The quenching will be important especially when coronal brain slices of older mice will be stained since the formation of lipofuscin particles is known to occur during the process of ageing (94). In addition, it will be relevant to stain coronal brain slices of mice at different ages, to investigate potential changes in the ORF1p expression with ageing.

However, to validate the specificity of the ORF1p antibody, it would be relevant to create upregulation or downregulation of the ORF1p. On the one hand, upregulation of LINE-1 retrotransposition activity can be achieved by injecting 6-hydroxydopamine in the mouse brain. As a result, oxidative stress will be provoked associated with an increase in LINE-1 retrotransposition and thus an increase in the ORF1p expression (67). When the brain of these mice will be stained, a higher expression of the ORF1p should be observed. On the other hand, downregulation of the ORF1p is another possibility to validate the

specificity of the antibody. However, it is estimated that the mouse genome consists of 3000 active LINE-1 copies making it hard to create a knock-out of all these elements (95).

Taking the advantage of immunofluorescent staining into account, it is possible to use multiple primary antibodies in one single experiment. Therefore, a staining with antibodies against ORF1p, tyrosine hydroxylase and neuronal nuclear protein could be performed. This will allow the identification of the subcellular localisation of the ORF1p in TH positive and TH negative neurons. In addition, a quantitative analysis could give an estimation of the difference in expression levels of the ORF1p in these different type of neurons.

The optimization of the ORF1p staining in this master thesis makes it possible to investigate the relation between LINE-1 and PD in the future. The endogenous expression of the ORF1p was revealed in WT mice, allowing to compare the ORF1p expression levels in different PD mouse models. In analogy with the upregulation of the ORF1p in *En1*-het mice, we may also observe an upregulation in other PD mouse models. Future research has to corroborate the role of LINE-1 in the pathogenesis of PD.

6 REFERENCES

1. Elbarbary RA, Lucas BA, et al. Retrotransposons as regulators of gene expression. Science. 2016;351(6274).
2. Kazazian HH, Moran JV. Mobile DNA in Health and Disease. N Engl J Med. 2017;377(4):361-70.
3. Cordaux R, Batzer MA. The impact of retrotransposons on human genome evolution. Nat Rev Genet. 2009;10(10):691-703.
4. Hancks DC, Kazazian H. Roles for retrotransposon insertions in human disease. Mob DNA. 2016;7(1):9.
5. McClintock B. The origin and behavior of mutable loci in maize. Genetics. 1950;36:344-55.
6. Dombroski B, Mathias S, et al. Isolation of an active human transposable element. Science. 1991;254(5039):1805-8.
7. Munoz-Lopez M, Garcia-Perez JL. DNA transposons: nature and applications in genomics. Curr Genomics. 2010;11:115-28.
8. Saleh A, Macia A, et al. Transposable Elements, Inflammation, and Neurological Disease. Front Neurol. 2019;10:894.
9. Scott EC, Devine SE. The Role of Somatic L1 Retrotransposition in Human Cancers. Viruses. 2017;9(6).
10. Brouha B, Schustak J, et al. Hot L1s account for the bulk of retrotransposition in the human population. PNAS. 2003;100(9):5280-5.
11. Krestel H, Meier JC. RNA Editing and Retrotransposons in Neurology. Front Mol Neurosci. 2018;11:163.
12. Rice GI, Meyzer C, et al. Reverse-Transcriptase Inhibitors in the Aicardi–Goutières Syndrome. N Engl J Med. 2018;379(23):2275-7.
13. Ariumi Y. Guardian of the Human Genome: Host Defense Mechanisms against LINE-1 Retrotransposition. Front Chem. 2016;4:28.
14. Beck CR, Garcia-Perez JL, et al. LINE-1 elements in structural variation and disease. Annu Rev Genomics Hum Genet. 2011;12:187-215.
15. Denli AM, Narvaiza I, et al. Primate-specific ORF0 contributes to retrotransposon-mediated diversity. Cell. 2015;163(3):583-93.
16. Lavie L, Maldener E, et al. The human L1 promoter: variable transcription initiation sites and a major impact of upstream flanking sequence on promoter activity. Genome Res. 2004;14(11):2253-60.
17. Richardson SR, Doucet AJ, et al. The Influence of LINE-1 and SINE Retrotransposons on Mammalian Genomes. Microbiol Spectr. 2015;3(2).
18. Terry DM, Devine SE. Aberrantly High Levels of Somatic LINE-1 Expression and Retrotransposition in Human Neurological Disorders. Front Genet. 2019;10:1244.
19. Muotri AR, Chu VT, et al. Somatic mosaicism in neuronal precursor cells mediated by L1 retrotransposition. Nature. 2005;435(7044):903-10.
20. Muotri AR, Zhao C, et al. Environmental influence on L1 retrotransposons in the adult hippocampus. Hippocampus. 2009;19(10):1002-7.
21. Coufal NG, Garcia-Perez JL, et al. L1 retrotransposition in human neural progenitor cells. Nature. 2009;460(7259):1127-31.
22. Suarez NA, Macia A, et al. LINE-1 retrotransposons in healthy and diseased human brain. Dev Neurobiol. 2018;78(5):434-55.
23. Macia A, Widmann TJ, et al. Engineered LINE-1 retrotransposition in nondividing human neurons. Genome Res. 2017;27(3):335-48.
24. Baillie JK, Barnett MW, et al. Somatic retrotransposition alters the genetic landscape of the human brain. Nature. 2011;479(7374):534-7.

25. Evrony GD, Cai X, et al. Single-neuron sequencing analysis of L1 retrotransposition and somatic mutation in the human brain. Cell. 2012;151(3):483-96.

26. Upton KR, Gerhardt DJ, et al. Ubiquitous L1 mosaicism in hippocampal neurons. Cell. 2015;161(2):228-39.

27. Kopera HC, Larson PA, et al. LINE-1 Cultured Cell Retrotransposition Assay. Methods Mol Biol. 2016;1400:139-56.

28. Rangwala SH, Kazazian HH, Jr. The L1 retrotransposition assay: a retrospective and toolkit. Methods. 2009;49(3):219-26.

29. Moran JV, Holmes SE, et al. High Frequency Retrotransposition in Cultured Mammalian Cells. Cell Press. 1996;87:917-27.

30. Raiz J, Damert A, et al. The non-autonomous retrotransposon SVA is trans-mobilized by the human LINE-1 protein machinery. Nucleic Acids Res. 2012;40(4):1666-83.

31. Ostertag EM, Luning ET, et al. Determination of L1 retrotransposition kinetics in cultured cells. Nucleic Acids Research. 2000;28(6):1418-23.

32. Del Re B, Marcantonio P, et al. Evaluation of LINE-1 mobility in neuroblastoma cells by in vitro retrotransposition reporter assay: FACS analysis can detect only the tip of the iceberg of the inserted L1 elements. Exp Cell Res. 2010;316(20):3358-67.

33. Kempen MHC, Bodea GO, et al. Neuronal Genome Plasticity: Retrotransposons, Environment and Disease. In: Cristofari G, editor. Human Retrotransposons in Health and Disease. Cham: Springer International Publishing; 2017. p. 107-25.

34. Sanchez-Luque FJ, Richardson SR, et al. Retrotransposon Capture Sequencing (RC-Seq): A Targeted, High-Throughput Approach to Resolve Somatic L1 Retrotransposition in Humans. In: Garcia-Pérez JL, editor. Transposons and Retrotransposons: Methods and Protocols. New York, NY: Springer New York; 2016. p. 47-77.

35. Tausig F, Wolf FJ. Streptavidin - a substance with avidin-like properties produced by microorganisms. Biochem Biophys Res Commun. 1964;14(3):205-9.

36. Thomas CA, Paquola AC, et al. LINE-1 retrotransposition in the nervous system. Annu Rev Cell Dev Biol. 2012;28:555-73.

37. Graham V, Khudyakov J, et al. SOX2 Functions to Maintain Neural Progenitor Identity. Neuron. 2003;39(5):749-65.

38. Muotri AR, Marchetto MC, et al. L1 retrotransposition in neurons is modulated by MeCP2. Nature. 2010;468(7322):443-6.

39. Lennartsson A, Arner E, et al. Remodeling of retrotransposon elements during epigenetic induction of adult visual cortical plasticity by HDAC inhibitors. Epigenetics & Chromatin. 2015;8(1).

40. Van Meter M, Kashyap M, et al. SIRT6 represses LINE1 retrotransposons by ribosylating KAP1 but this repression fails with stress and age. Nat Commun. 2014;5:5011.

41. Tedeschi A, Di Giovanni S. The non-apoptotic role of p53 in neuronal biology: enlightening the dark side of the moon. EMBO Rep. 2009;10(6):576-83.

42. Wylie A, Jones AE, et al. p53 genes function to restrain mobile elements. Genes Dev. 2016;30(1):64-77.

43. Kuwabara T, Hsieh J, et al. Wnt-mediated activation of NeuroD1 and retro-elements during adult neurogenesis. Nat Neurosci. 2009;12(9):1097-105.

44. Athanikar JN, Badge RM, et al. A YY1-binding site is required for accurate human LINE-1 transcription initiation. Nucleic Acids Res. 2004;32(13):3846-55.

45. Tchénio T, Casella JF, et al. Members of the SRY family regulate the human LINE retrotransposons. Nucleic Acids Res. 2000;28(2):411-5.

46. Yang N, Zhang L, et al. An important role for RUNX3 in human L1 transcription and retrotransposition. Nucleic Acids Res. 2003;31(16):4929-40.

47. Shi X, Seluanov A, et al. Cell divisions are required for L1 retrotransposition. Mol Cell Biol. 2007;27(4):1264-70.

48. Idica A, Sevrioukov EA, et al. MicroRNA miR-128 represses LINE-1 (L1) retrotransposition by down-regulating the nuclear import factor TNPO1. J Biol Chem. 2017;292(50):20494-508.

49. Twyffels L, Gueydan C, et al. Transportin-1 and Transportin-2: protein nuclear import and beyond. FEBS Lett. 2014;588(10):1857-68.

50. Kataoka N, Bachorik JL, et al. Transportin-SR, a nuclear import receptor for SR proteins. J Cell Biol. 1999;145(6):1145-52.

51. Lai MC, Lin RI, et al. A human importin-beta family protein, transportin-SR2, interacts with the phosphorylated RS domain of SR proteins. J Biol Chem. 2000;275(11):7950-7.

52. Fu X. The superfamily of arginine/serine-rich splicing factors. RNA. 1995;1(7):663-80.

53. Christ F, Thys W, et al. Transportin-SR2 imports HIV into the nucleus. Curr Biol. 2008;18(16):1192-202.

54. Fernandez J, Machado AK, et al. Transportin-1 binds to the HIV-1 capsid via a nuclear localization signal and triggers uncoating. Nat Microbiol. 2019;4(11):1840-50.

55. Zhang X, Zhang R, et al. New Understanding of the Relevant Role of LINE-1 Retrotransposition in Human Disease and Immune Modulation. Front Cell Dev Biol. 2020;8:657.

56. Savitsky K, Bar-Shira A, et al. A single ataxia telangiectasia gene with a product similar to PI-3 kinase. Science. 1995;268(5218):1749-53.

57. Bar-Shira A, Rashi-Elkeles S, et al. ATM-dependent activation of the gene encoding MAP kinase phosphatase 5 by radiomimetic DNA damage. Oncogene. 2002;21(5):849-55.

58. Coufal NG, Garcia-Perez JL, et al. Ataxia telangiectasia mutated (ATM) modulates long interspersed element-1 (L1) retrotransposition in human neural stem cells. PNAS. 2011;108(51):20382-7.

59. Blennow K, de Leon MJ, et al. Alzheimer's disease. The Lancet. 2006;368(9533):387-403.

60. Tam OH, Ostrow LW, et al. Diseases of the nERVous system: retrotransposon activity in neurodegenerative disease. Mob DNA. 2019;10:32.

61. Bollati V, Galimberti D, et al. DNA methylation in repetitive elements and Alzheimer disease. Brain Behav Immun. 2011;25(6):1078-83.

62. Hernández HG, Mahecha MF, et al. Global Long Interspersed Nuclear Element 1 DNA Methylation in a Colombian Sample of Patients With Late-Onset Alzheimer's Disease. Am J Alzheimers Dis Other Demen. 2013;29(1):50-3.

63. Searles Nielsen S, Checkoway H, et al. LINE-1 DNA methylation, smoking and risk of Parkinson's disease. J Parkinsons Dis. 2012;2(4):303-8.

64. Davie CA. A review of Parkinson's disease. Br Med Bull. 2008;86:109-27.

65. Desplats P, Spencer B, et al. Alpha-synuclein sequesters Dnmt1 from the nucleus: a novel mechanism for epigenetic alterations in Lewy body diseases. J Biol Chem. 2011;286(11):9031-7.

66. Di Lorenzo Alho AT, Suemoto CK, et al. Three-dimensional and stereological characterization of the human substantia nigra during aging. Brain Struct Funct. 2016;221(7):3393-403.

67. Blaudin de The FX, Rekaik H, et al. Engrailed homeoprotein blocks degeneration in adult dopaminergic neurons through LINE-1 repression. EMBO J. 2018;37(15).

68. Rekaik H, Blaudin de Thé F-X, et al. Engrailed Homeoprotein Protects Mesencephalic Dopaminergic Neurons from Oxidative Stress. Cell Rep. 2015;13(2):242-50.

69. Sonnier L, Le Pen G, et al. Progressive loss of dopaminergic neurons in the ventral midbrain of adult mice heterozygote for Engrailed1. J Neurosci. 2007;27(5):1063-71.

70. Zhang XM, Yin M, et al. Cell-based assays for Parkinson's disease using differentiated human LUHMES cells. Acta Pharmacol Sin. 2014;35(7):945-56.

71. Scholz D, Poltl D, et al. Rapid, complete and large-scale generation of post-mitotic neurons from the human LUHMES cell line. J Neurochem. 2011;119(5):957-71.

72. Baeken MW, Moosmann B, et al. Retrotransposon activation by distressed mitochondria in neurons. Biochem Biophys Res Commun. 2020;525(3):570-5.

73. Pfaff AL, Bubb VJ, et al. An Increased Burden of Highly Active Retrotransposition Competent L1s Is Associated with Parkinson's Disease Risk and Progression in the PPMI Cohort. Int J Mol Sci. 2020;21(18).

74. Dai L, Huang Q, et al. Effect of reverse transcriptase inhibitors on LINE-1 and Ty1 reverse transcriptase activities and on LINE-1 retrotransposition. BMC Biochem. 2011;12:18.

75. Nguyen Van Nhien A, Tomassi C, et al. First Synthesis and Evaluation of the Inhibitory Effects of Aza Analogues of TSAO on HIV-1 Replication. J Med Chem. 2005;48:4276-84.

76. Arts EJ, Wainberg MA. Mechanisms of Nucleoside Analog Antiviral Activity and Resistance during Human Immunodeficiency Virus Reverse Transcription. Antimicrob Agents Chemother. 1996;40(3):527-40.

77. De Clercq E. HIV resistance to reverse transcriptase inhibitors. Biochem Pharmacol. 1994;47(2):155-69.

78. De Clercq E. HIV-1-specific RT inhibitors: Highly selective inhibitors of human immunodeficiency virus type 1 that are specifically targeted at the viral reverse transcriptase. Med Res Rev. 1993;13(3):229-58.

79. Merluzzi V, Hargrave K, et al. Inhibition of HIV-1 replication by a nonnucleoside reverse transcriptase inhibitor. Science. 1990;250(4986):1411-3.

80. Sluis-Cremer N, Tachedjian G. Mechanisms of inhibition of HIV replication by non-nucleoside reverse transcriptase inhibitors. Virus Res. 2008;134(1-2):147-56.

81. Jones RB, Garrison KE, et al. Nucleoside analogue reverse transcriptase inhibitors differentially inhibit human LINE-1 retrotransposition. PLoS One. 2008;3(2):e1547.

82. Banuelos-Sanchez G, Sanchez L, et al. Synthesis and Characterization of Specific Reverse Transcriptase Inhibitors for Mammalian LINE-1 Retrotransposons. Cell Chem Biol. 2019;26(8):1095-109

83. Crow YJ, Manel N. Aicardi-Goutieres syndrome and the type I interferonopathies. Nat Rev Immunol. 2015;15(7):429-40.

84. Crow YJ, Hayward BE, et al. Mutations in the gene encoding the 3'-5' DNA exonuclease TREX1 cause Aicardi-Goutieres syndrome at the AGS1 locus. Nat Genet. 2006;38(8):917-20.

85. Rice GI, Bond J, et al. Mutations involved in Aicardi-Goutieres syndrome implicate SAMHD1 as regulator of the innate immune response. Nat Genet. 2009;41(7):829-32.

86. Reyniers L, Del Giudice MG, et al. Differential protein-protein interactions of LRRK1 and LRRK2 indicate roles in distinct cellular signaling pathways. J Neurochem. 2014;131(2):239-50.

87. Sariyer IK. Transfection of neuronal cultures. Methods Mol Biol. 2013;1078:133-9.

88. Wiesenhofer B, Kaufmann WA, et al. Improved lipid-mediated gene transfer in C6 glioma cells and primary glial cells using FuGENE™. J Neurosci Methods. 1999;92:145-52.

89. Kovalevich J, Langford D. Considerations for the use of SH-SY5Y neuroblastoma cells in neurobiology. Methods Mol Biol. 2013;1078:9-21.

90. Gresch O, Engel FB, et al. New non-viral method for gene transfer into primary cells. Methods. 2004;33(2):151-63.

91. Hamdorf M, Idica A, et al. miR-128 represses L1 retrotransposition by binding directly to L1 RNA. Nat Struct Mol Biol. 2015;22(10):824-31.

92. Kubo S, Seleme MdC, et al. L1 retrotransposition in nondividing and primary human somatic cells. Proceedings of the National Academy of Sciences. 2006;103:8036-41.

93. Di Guardo G. Lipofuscin, lipofuscin-like pigments and autofluorescence. Eur J Histochem. 2015;59(1):2485.

94. Terman A, Brunk UT. Lipofuscin: Mechanisms of formation and increase with age. APMIS. 1998;106:265-76.

95. Goodier JL, Ostertag EM, et al. A novel active L1 retrotransposon subfamily in the mouse. Genome Res. 2001;11(10):1677-85.